



Published in final edited form as:

Curr Med Chem. 2016 ; 23(3): 201–241.

Derivatives of Procaspace-Activating Compound 1 (PAC-1) and Anticancer Activities

Howard S. Roth and Paul J. Hergenrother*

Department of Chemistry, University of Illinois, Urbana, IL, USA

Abstract

PAC-1 induces the activation of procaspase-3 *in vitro* and in cell culture by chelation of inhibitory labile zinc ions via its *ortho*-hydroxy-*N*-acylhydrazone moiety. First reported in 2006, PAC-1 has shown promise in cell culture and animal models of cancer, and a Phase I clinical trial in cancer patients began in March 2015 (NCT02355535). Because of the considerable interest in this compound and a well-defined structure-activity relationship, over 1000 PAC-1 derivatives have been synthesized in an effort to vary pharmacological properties such as potency and pharmacokinetics. This article provides a comprehensive examination of all PAC-1 derivatives reported to date. A survey of PAC-1 derivative libraries is provided, with an in-depth discussion of four derivatives on which extensive studies have been performed.

Keywords

PAC-1; procaspase-3; zinc; apoptosis; cancer; library

1. INTRODUCTION

Apoptosis is a form of programmed cell death by which cells that are damaged, in excess, or otherwise no longer needed are removed in a controlled manner. The caspase cascade is central to this process, as these cysteine proteases are cleaved from their proenzyme forms in response to proapoptotic stimuli. [1, 2] In particular, the cleavage of procaspase-3 to caspase-3 represents a critical node in apoptosis, as this executioner caspase catalyzes the hydrolysis of hundreds of protein substrates, [3–6] leading to cell death. A key hallmark of cancer is the ability of tumor cells to evade apoptosis through mutation and misregulation of apoptotic proteins. [7, 8] As a result, several anticancer drug discovery strategies have focused on the direct targeting of these aberrant proteins; these mutated and upregulated proteins often exist at much higher concentrations in tumors than in healthy tissues, and thus, in principle, undesired apoptosis in normal cells can be minimized. Specifically, considerable effort has been invested in the small molecule-mediated inhibition of antiapoptotic proteins, including MDM2, [9, 10] Bcl-2, [11, 12] and XIAP [13, 14] (Figure 1). A complementary approach involves the small molecule-mediated *activation* of

*Address correspondence to this author at the Department of Chemistry, University of Illinois, 261 Roger Adams Laboratory, Box 36-5, 600 S. Mathews Ave., Urbana, IL, 61801, USA; Tel: +1-217-333-0363; Fax: +1-217-244-8024; hergenro@illinois.edu.

CONFLICT OF INTEREST

The University of Illinois has filed patents on some of the compounds described in this article.

proapoptotic proteins, including procaspase-3. [15–18] Based on the downstream location of procaspase-3 in the apoptotic cascade relative to frequently mutated proteins, [2] the low frequency of procaspase-3 mutations in cancer, [19] and the robust expression of the procaspase-3 enzyme in a number of cancer types, including lymphoma, [20, 21] leukemia, [22, 23] multiple myeloma, [24] melanoma, [25, 26] glioblastoma, [27, 28] pancreatic cancer, [29] liver cancer, [30] lung cancer, [31–33] breast cancer, [34–37] esophageal cancer, [38] and colon cancer, [15, 39–41] the small molecule-mediated activation of procaspase-3 is actively being explored as an anticancer strategy. [15–18]

2. PAC-1

2.1. Initial discovery of PAC-1

In a high-throughput screen of over 20,000 small molecules, Procaspase Activating Compound 1 (**PAC-1**, **1**, Figure 2) was identified as a compound that could enhance the enzymatic activity of procaspase-3 *in vitro*. [15] **PAC-1** and its derivatives induce apoptosis and are cytotoxic in cell culture to a diverse array of cancer cells, including cell lines derived from white blood cell cancers (lymphoma, [15, 42–51] leukemia, [15, 24, 44, 48–50, 52–55] and multiple myeloma [24, 55]), diverse carcinomas (breast, [15, 44, 48, 49, 52–54, 56–59] renal, [15] adrenal, [15, 60–62] colon, [15, 48, 55, 57–59, 63] lung, [15, 48, 49, 52–59, 63–67] cervical, [44, 55] gastric, [48, 49, 55, 57, 58, 63] ovarian, [55] liver, [48, 49, 55] prostate, [48, 49] and gallbladder [48, 49]), and other solid tumor types (melanoma, [15, 44, 48, 49] osteosarcoma, [55] neuroblastoma, [15, 55, 57, 58] and glioblastoma [48, 49, 68]). Patient-derived samples from colon cancer [15], chronic lymphocytic leukemia [23], and multiple myeloma [24] are also sensitive to **PAC-1** and derivatives, and a therapeutic effect has been demonstrated in multiple murine tumor models [15, 48, 49, 56, 65, 66, 69] and in pet dogs with cancer. [44] In addition, **PAC-1** displays potent synergy with the antitumor agent paclitaxel, [65, 66, 69] as well as **1541B**, [56] the second reported procaspase-3 activator, [16, 70–72] in various cell culture and *in vivo* models of cancer, and a derivative of **PAC-1** showed synergy with an investigational Smac mimetic in cell culture. [23]

An initial evaluation of **PAC-1** structure-activity relationships (SAR) was undertaken with a small number of closely related compounds and synthetic intermediates (Figure 2). **PAC-1** was the most potent compound evaluated, while removal of the allyl group (**2**) led to a slight loss in potency. However, each of the other compounds studied (**3–10**) were inactive in both procaspase-3 activation and cytotoxicity assays. [15]

2.2. PAC-1 mechanism of action

One of the most informative results from the initial report on **PAC-1** was that removal of the hydroxyl group (compound **3**, also known as **PAC-1a**) abolished activity. This established the essential nature of the phenolic hydroxyl and suggested further examination of the *ortho*-hydroxy-*N*-acylhydrazone moiety for its relationship to the anticancer activity of **PAC-1**. Complexes of *ortho*-hydroxy-*N*-acylhydrazones with metals, including iron, [73] copper, [74] and zinc, [75] are well known, and inhibition of procaspase [42] and caspase [76–79] enzymes by divalent metal cations is well established. In particular, zinc from the labile zinc pool, which is bound loosely to certain proteins, co-localizes with procaspase-3 [80] and

zinc inhibits the enzymatic activity of both procaspase-3 [42] and caspase-3, [77] as illustrated in Figure 1. In addition, a putative binding site on procaspase-3/caspase-3 for labile zinc ions has been identified. [81] The role of zinc in the mechanism of action of **PAC-1** has been extensively investigated. [42] **PAC-1** binds zinc in a 1:1 ratio with a K_d of 52 ± 2 nM. [42, 43] **PAC-1** shows no activity toward procaspase-3 in a metal-free buffer; however, the addition of zinc inhibits procaspase-3 activity, and **PAC-1** restores this activity in a dose-dependent manner through chelation of the inhibitory zinc (Figure 3A). In addition, **PAC-1** induces apoptosis in U-937 (human lymphoma) cells, but the addition of zinc to the cell culture medium abolishes the ability of **PAC-1** to induce apoptosis. [42] Finally, **PAC-1a** (lacking the phenolic hydroxyl) displays no affinity toward zinc and is unable to induce procaspase-3 activation. Based on these results, a mechanism of action has been proposed for **PAC-1** activity (Figure 3B): zinc binds loosely to procaspase-3 (dissociation constants of high nM to low μ M), [81] inhibiting its activity. With a low- to mid-nM affinity for zinc, [42, 43, 50] **PAC-1** efficiently competes with procaspase-3 for the loosely-bound zinc ions. This depletion of the labile zinc pool restores procaspase-3 enzymatic activity, allowing for cleavage of procaspase-3 to caspase-3 and the initiation of the execution pathway of apoptosis. [42] **PAC-1** is now widely used as a tool compound for the induction of apoptosis [51, 59, 67, 68, 82, 83], and for the direct activation of procaspase-3 downstream of the mitochondria. [84–87] In addition, multiple independent studies have confirmed the direct procaspase-3 activation mechanism, [48, 85, 88] for example in detailed studies with selective caspase inhibitors, [85] selective caspase substrates, [48] and in Bax/Bak double knockout cells. [88] The effect of procaspase-3 activators has been shown to be influenced by growth factors in the PC12 cell line. [61]

The affinity of **PAC-1** for zinc is not strong enough to disrupt proteins containing essential zinc ions; **PAC-1** and several derivatives show no inhibitory activity toward “classic” zinc-containing metalloenzymes including matrix metalloproteinases-9 and -14, [89] as well as carboxypeptidase A and histone deacetylase. [23] A thorough discussion of the relationship between **PAC-1** and other therapeutically relevant metal chelators was reported recently. [50] The considerable evidence suggesting that **PAC-1** does not belong in the category of so-called Pan-Assay Interference Compounds (PAINS) [90] has also been extensively discussed. [50]

2.3. Structure-activity relationships

With a preliminary understanding of the mechanism of action of **PAC-1**, SAR studies of the compound were initiated by the Hergenrother laboratory. [43] In order to investigate the SAR, four classes of **PAC-1** derivatives were designed (Figure 4). Class I derivatives (**2**, **3**, **11a–h**, and **12**) contained modifications to the benzylidene group, Class II derivatives (**13a–c** and **14a–d**) contained modifications to the benzyl group, and the single Class III derivative (**15**) contained modifications to both aromatic rings. Class IV derivatives (**16a–b**, **17a–b**, **18**, **19**, and **20**) contained modifications to the four nitrogen atoms present in **PAC-1**. In total, 26 derivatives were synthesized and compared to **PAC-1** in a series of experiments. [43]

The results from evaluation of the compounds are shown in Table 1. Compounds were evaluated for their ability to chelate zinc, relieve zinc-mediated inhibition of caspase-3, and

induce cell death in U-937 cells. These experiments confirmed the essential nature of the *ortho*-hydroxy-*N*-acylhydrazone for activity. Class I derivatives lacking the phenol showed significantly reduced activity compared to **PAC-1** in these experiments, while the two Class I derivatives containing the phenol (**2** and **11g**) retained activity. However, modification of the benzyl group was tolerated, as Class II derivatives showed similar activity to **PAC-1**. The Class III derivative (**15**) was also active, suggesting that substitution of both aromatic rings could be tolerated, as long as the *ortho*-hydroxy-*N*-acylhydrazone remained intact. Class IV derivatives that contained the *ortho*-hydroxy-*N*-acylhydrazone (**16a–b** and **18**) were capable of binding zinc and inducing cell death, although compounds **16a–b** showed inhibitory activity toward caspase-3. Class IV derivatives containing modifications to the hydrazone (**17a–b**, **19**, and **20**) showed diminished activity relative to **PAC-1**. In order to further investigate the cellular effects of **PAC-1** and derivatives, U-937 cells were treated with **PAC-1**, **14a**, or **18** at 50 μ M for 12 hours, and cell death was assessed by flow cytometry with Annexin V-FITC/propidium iodide staining. Large populations of Annexin V-FITC positive, propidium iodide negative cells were present for each compound treatment, indicating that cell death induced by these compounds proceeds through apoptosis. [43]

An additional derivative of **PAC-1** was synthesized containing a fluorophore conjugated to the benzyl ring through a triazole linker. This compound (**AF350-PAC-1**, **21**, Figure 5) was found to bind zinc, activate caspase-3 *in vitro*, and induce cell death in culture. SK-MEL-5 cells were treated with **21** and FAM-DEVD-fmk, an inhibitor of caspases-3 and -7 that covalently modifies the enzymes with a fluorophore. FAM-DEVD-fmk therefore represents a marker for sites of caspase-3/-7 activity within cells. Cells were treated for one hour, washed in phenol red-free medium, and incubated for an additional two hours. The cells were then visualized at emission wavelengths of 400 nm (**21**) and 520 nm (FAM-DEVD-fmk). Treatment of cells with vehicle showed minimal fluorescence in either channel. Minimal increases in fluorescence were observed upon treatment with FAM-DEVD-fmk alone. Treatment with **21** alone showed punctate staining in the cytoplasm at 400 nm. Finally, cells treated with both **21** and FAM-DEVD-fmk showed punctate staining at both 400 nm and 520 nm, and the merged image showed overlap for the majority of these sites of fluorescence. This overlap strongly supports the notion that **21** induces activation of executioner caspases in cells and co-localizes with sites of caspase-3/-7 activity. [43]

3. PAC-1 DERIVATIVE LIBRARIES

3.1. Diaryl urea conjugates

With the goal of improving upon **PAC-1**, several classes of derivatives have been synthesized and evaluated. One approach toward improving the potency of **PAC-1** explored by Gong and coworkers involved the conjugation of fragments derived from sorafenib (**22**), a diaryl urea that inhibits several kinases, including VEGFR, PDGFR, and B-Raf, to **PAC-1**. [52–54] Initially, two series of compounds were synthesized (Table 2). [52] In the first series (**23a–k**), diaryl ureas were conjugated via a thiazole to the piperazine/*ortho*-hydroxy-*N*-acylhydrazone portion of **PAC-1**, and substituents on each terminal arene were varied. In the second series (**24a–g**), the phenol ring was replaced with a hydantoin. The cytotoxicity of the 18 compounds was evaluated in A549 (human lung), HL-60 (human leukemia), and

MDA-MB-231 (human breast) cancer cell lines in culture and compared to **PAC-1** and sorafenib. In general, the compounds of series **23** were much more potent than the compounds of series **24**, confirming the essential nature of the *ortho*-hydroxy-*N*-acylhydrazone for activity of **PAC-1** derivatives. Many of the compounds of series **23** were more potent than **PAC-1** or sorafenib, suggesting the potential for improved potency via dual pharmacophores.

Building upon these results, a second set of 18 diaryl urea/**PAC-1** conjugates was synthesized (Table 3). [53] Because the hydantoin derivatives were significantly less active, synthesis of derivatives was limited to those containing the *ortho*-hydroxy-*N*-acylhydrazone moiety. Nine additional derivatives of the compound **23** series (**23l-t**) were synthesized. In addition, nine derivatives (**25a-i**) were synthesized that contained an amide linkage instead of the thiazole. These compounds were also evaluated in A549, HL-60, and MDA-MB-231 cells in culture and compared to **PAC-1** and sorafenib. Most of the compounds displayed comparable potency to both of the parent compounds in the cell lines tested. In general, the compounds from series **23** were somewhat more potent than the compounds from series **25**. The addition of a benzyloxy substituent to the benzylidene ring increased potency for compounds of the **23** series. Three of the derivatives (**23l**, **23q**, and **23s**), as well as **PAC-1** and sorafenib, were evaluated in a human embryonic lung fibroblast-derived cell line (WI-38) in culture. The compounds exhibited slightly reduced potency in this cell line compared to the cancer cell lines, suggesting a degree of selectivity for toxicity to cancer cells over normal cells in culture. [53]

The final set of 26 diaryl urea/**PAC-1** conjugates is shown in Table 4. This set of compounds included 23 phenol derivatives (**23u-qq**) and three hydantoin derivatives (**24h-j**), conjugated to the diaryl urea moiety via a thiazole linker. [54] The compounds were evaluated in A549, HL-60, and MDA-MB-231 cells in a 72-hour cytotoxicity assay and compared to **PAC-1** and sorafenib. The compounds of the hydantoin series were again observed to be less potent than the compounds of the phenol series. Within the phenol series, the coumarin derivatives (**23mm-qq**) were less potent than the other derivatives. Many of the substituted phenol derivatives had sub-micromolar potency in the cell lines, improving upon the activity of either parent compound alone, and the benzyloxy derivatives were among the most potent compounds in this library. This provides additional validation that the conjugation of other cytotoxic agents to **PAC-1** can help to increase the potency of either agent alone. [54]

3.2. Benzothiazole **PAC-1** derivatives

Building on the promising results from the phenylthiazole-containing **PAC-1** derivatives, two series of benzothiazole-conjugated semicarbazone **PAC-1** derivatives were synthesized by Gong and coworkers. [57, 58] The benzothiazole derivatives were substituted at the 6-position to block metabolism. Positively-charged substituents were chosen in order to mimic the piperazine nitrogen atoms present in **PAC-1**. [57, 58] The first series (Table 5) contained 26 derivatives (**26a-z**). [57] Cytotoxicity of the compounds was evaluated over 72 hours in HT-29 (human colon cancer), MDA-MB-231 (human breast cancer), MKN-45 (human gastric cancer), NCI-H226 (human lung cancer), and SK-N-SH (human neuroblastoma) cell

lines in culture. Many of the compounds were found to display equal or greater potency compared to **PAC-1**. As with the diaryl urea conjugates, the benzyloxy substituent increased potency, while the coumarin-derived compounds were less potent. Importantly, the semicarbazone proved to be an acceptable replacement for the hydrazone of **PAC-1**, as compounds retained potency in the cell lines tested. [57]

Based on these results, a second set of benzothiazole **PAC-1** derivatives was designed (Table 6). [58] These 36 compounds (**26aa–jjj**) were also linked via the semicarbazone and contained basic substituents at the 6 position of the benzothiazole. Several of the compounds (**26ii–fff**) contained the benzyloxy group that helped to improve potency for the first series of benzothiazole derivatives. In four derivatives (**26ggg–jjj**) the phenyl of the benzyloxy was modified to a piperonylthiazole moiety, a motif present in the **PAC-1** derivatives **WF-210** and **WF-208**. [48, 49] The compounds were evaluated in a 72-hour cell culture assay against the five cell lines previously discussed. All compounds were potent in the cytotoxicity assays, with many exhibiting sub-micromolar IC_{50} values. As previously, the compounds containing the benzyloxy substituents were among the most potent compounds in the library, and the piperonylthiazole derivatives were also potent in cell culture. Compounds containing the morpholino substituent were somewhat less potent than other derivatives. In addition, there was a general correlation between potency and intracellular procaspase-3 concentration; NCI-H226 cells express procaspase-3 to a much greater degree than SK-N-SH cells, and the compounds were more potent in the NCI-H226 cells than the SK-N-SH cells. This provides further support to the proposed mechanism of action of **PAC-1**. [58]

3.3. Oxadiazole **PAC-1** derivatives

In addition to the benzothiazole-containing compounds, several **PAC-1** derivatives (**27a–s**) were synthesized by Gong, Wu, and coworkers, containing an oxadiazole with a substituted (phenoxyethyl)phenyl linked to the piperazine ring (Table 7). [48, 49] The *ortho*-hydroxy-*N*-acylhydrazone remained intact, while substitution varied on the benzylidene ring. Four derivatives (**27a–d**) contained the 3-allyl substituent characteristic of **PAC-1**. An additional 12 derivatives (**27e–p**) contained a substituted benzyloxy group at the 4-position of the benzylidene ring. Finally, three derivatives (**27q–s**) contained a piperonyl substituent attached via a thiazole linker. The cytotoxicity of the compounds to HL-60 cells was evaluated in a 72-hour experiment. **PAC-1** had an IC_{50} value of 2.10 μ M under these conditions, and most of the derivatives were more potent than **PAC-1** in the HL-60 cell line, although compound **27p** was inactive in this experiment. In general, the compounds containing the allyl and the piperonylthiazole substituents were more potent than those containing the benzyloxy substituents. Compounds **27r–s** (also called **WF-210** and **WF-208**, respectively) showed considerable potency in cell culture, with 80 nM IC_{50} values, and further experiments were performed with these two derivatives, as discussed in Section 5. [48, 49]

3.4. Replacement of benzylidene

PAC-1 chelates zinc with affinity in the low nanomolar range, [42, 43] which is strong enough to remove the labile pool of zinc, but not strong enough to disrupt essential zinc ions. [23, 89] In contrast, **TPEN** (**28**, Figure 6), which binds zinc with 0.26 fM affinity, [91]

inhibits the activity of certain metalloenzymes via chelation of the essential metal ion. [92] It is likely that the relatively modest affinity of **PAC-1** for zinc is responsible for its selectivity for chelation of labile zinc over essential zinc ions. In an effort to slightly increase the affinity of **PAC-1** for zinc, two new **PAC-1** derivatives were synthesized by Rongved and coworkers. [60] For **ZnA-DPA (29)**, the benzylidene was replaced by a dipicolylamine (DPA) moiety, which is present in **TPEN**. For **ZnA-Pyr (30)**, the phenol was replaced by a 4-pyridoxyl group, which also contains the *ortho*-hydroxyl substituent necessary for **PAC-1** activity. [60]

ZnA-Pyr was found to bind zinc in a dose-dependent manner, although a K_d value was not calculated. The binding of **ZnA-DPA** to zinc could not be assessed due to the lack of a chromophore. Dissociation constants for compounds analogous to **ZnA-DPA** and **ZnA-Pyr** were in the low nanomolar [93] and high femtomolar [94] ranges, respectively. **PAC-1**, **TPEN**, **ZnA-DPA**, and **ZnA-Pyr** were evaluated in PC-12 cells in a 24-hour experiment. **TPEN** was the most potent compound in inducing cell death, followed by **PAC-1**. Neither **ZnA-DPA** nor **ZnA-Pyr** induced greater than 40% cell death at concentrations up to 200 μM . All four compounds induced activation of caspases-3/-7 in whole cells, as measured by cleavage of the fluorogenic substrate (DEVD)₂-Rhodamine 110. The activity of **PAC-1** and **TPEN** in this experiment was slightly higher than **ZnA-DPA** and **ZnA-Pyr**. The addition of zinc or the caspase-3/-7 inhibitor Ac-DEVD-cmk reduced the amount of cell death induced by each agent, although zinc-mediated protection of cell death induced by **ZnA-DPA** was not statistically significant. [60] While it remains possible that an alternative zinc-binding motif could lead to an improved **PAC-1** derivative, this study shows that the DPA and pyridoxyl substituents are most likely not appropriate for this purpose.

3.5. Study of matrix metalloproteinase inhibition

In an effort to evaluate potential off-target effects of **PAC-1**, six derivatives (**31a–f**, Figure 7) were synthesized, and the ability of the compounds to inhibit zinc-dependent matrix metalloproteinases-9 and -14 was evaluated by Winberg and coworkers. [89] The compounds do not inhibit the enzymes at 5 μM . Slight inhibition is observed at the high concentration of 100 μM , which is outside of physiologically relevant ranges. IC_{50} values for **31a** and **31b** were calculated at >100 μM . [89] This relatively weak level of inhibition of the metalloenzymes provides further support that **PAC-1** and derivatives selectively chelate the labile pool of zinc selectively over tightly-bound zinc ions.

3.6. Modification of piperazine

An additional strategy to improve the potency of **PAC-1** involved modification of the piperazine to acyclic 1,2-ethylenediamine and 1,3-propylenediamine linkers (Table 8), as performed by Xiao, Yang, and coworkers. [64] These derivatives (**32a–l**, **33a–f**) retained the benzyl substituent, and all but two (**32d** and **32h**) of the 18 derivatives synthesized contained the *ortho*-hydroxy-*N*-acylhydrazone; substituents on both aromatic rings were varied to assess structure-activity relationships. The compounds were evaluated in HL-60 (human leukemia) and HLF (human embryonic lung fibroblast) cells over 72 hours and compared to **PAC-1**. Many of the compounds were highly potent against the HL-60 cells, with IC_{50} values below 1 μM , compared to **PAC-1** at $1.90 \pm 0.01 \mu\text{M}$. Notably, the two derivatives

lacking the *ortho*-hydroxyl group were significantly less potent, confirming the previously determined structure-activity relationships. Many of the compounds displayed comparable potency in the non-cancerous HLF cell line, suggesting that there may be a narrow therapeutic window for these compounds. Compound **33b** was ~100-fold less potent in the HLF cell line than the HL-60 cell line. For this reason, compound **33b** was selected for further study in a panel of 14 additional human cancer cell lines (Table 9).

Compound **33b** was more potent than **PAC-1** in all of the cancerous cell lines evaluated, suggesting that modification of the piperazine may be a useful strategy for the development of improved **PAC-1** derivatives. In this experiment, three cell lines (A-498, DU145, and MCF7) were insensitive to **PAC-1**, as IC₅₀ values were higher than 300 μM. [64] Of note, the MCF7 cell line does not express procaspase-3, [95] and detailed studies with isogenic cell line pairs (MCF7 and MCF7 with forced procaspase-3 expression) reveal that MCF7 cells with forced procaspase-3 expression are markedly more sensitivity to apoptotic induction by procaspase-3 activating compounds. [56]

3.7. Combinatorial library of 837 PAC-1 analogues

3.7.1. Library design and synthesis—In order to expand upon previously determined structure-activity relationships [43] and identify potent derivatives, a library of diverse **PAC-1** analogues was designed and synthesized. The late-stage condensation of a hydrazide and an aldehyde to form the key *N*-acylhydrazone is the final synthetic step in routes toward **PAC-1** and many other derivatives. [15, 43, 44, 46, 48, 49, 52–54, 57, 58, 60, 64, 89] Through this modular synthesis, many diverse compounds can be constructed from a relatively small number of building blocks. As shown in Figure 8, each of 31 hydrazides (**34**{ 1–31}) was condensed with each of 27 aldehydes (**35**{ 1–27}) to construct a library of 837 **PAC-1** analogues (**36**{ 1–31, 1–27}). Reactions proceeded until the aldehyde was fully consumed, and polystyrene-bound benzaldehyde was added to react with and remove the excess hydrazide. After full consumption of the hydrazide, the resulting resin-bound hydrazones were removed by filtration, giving library members with 91% average purity. [46]

3.7.2. Evaluation of library—The 837 **PAC-1** analogues were evaluated for their ability to induce apoptosis in U-937 (human lymphoma) cells in culture for 24 hours at a concentration of 20 μM; **PAC-1** displays moderate potency (~50% cell death) against this cell line under these conditions. Six compounds were confirmed to induce >80% cell death in this assay (**36**{ 2,7}, **36**{ 4,7}, **36**{ 18,7}, **36**{ 20,24}, **36**{ 25,7}, and **36**{ 28,7}; structures in Table 10). The ability of the compounds to induce dose-dependent cell death was evaluated in U-937 cells and compared to **PAC-1** and its derivative **S-PAC-1** (**37**, discussed in Section 4). All six of these compounds potently induced cell death in culture in a 72-hour treatment. [46] In a second experiment, U-937 cells were exposed to the compounds at a single concentration (7.5 μM) for 24 hours, and cell viability was assessed by flow cytometry analysis with Annexin V-FITC/propidium iodide staining (Table 10 and Figure 9). The majority of the compound-treated cells were in an early or late apoptotic state, and the novel analogues induced apoptosis to a greater degree than **PAC-1** under these conditions. [46]

The ability of compounds to relieve zinc-mediated inhibition of procaspase-3 *in vitro* was then evaluated (Table 10). Procaspase-3 was incubated with ZnSO₄, which reduces its enzymatic activity by >95%. [42, 43] All compounds were able to restore the enzymatic activity of procaspase-3 under these conditions (as assessed by the cleavage of the colorimetric caspase-3 substrate Ac-DEVD-pNA [96]), and five of the six hit compounds were more potent than **PAC-1**. [46] Compound **36** {18,7}, also known as **B-PAC-1**, was evaluated in patient-derived leukemia samples, [23] as well as multiple myeloma cell lines and primary isolates, [24] as discussed in Section 6.

The six compounds shown in Table 10 emerged from the evaluation of the combinatorial library; these compounds are two- to four-fold more potent than **PAC-1** at induction of cancer cell death in both 24-hour and 72-hour assays. Of note, five of the six hit compounds contain two *tert*-butyl substituents on the benzylidene ring, while the sixth contains a *tert*-butyl substituent on the benzyl ring. There are several marketed drugs containing aryl *tert*-butyl groups, including the antihistamine buclizine, the CFTR potentiator ivacaftor for the treatment of cystic fibrosis, and the mutant B-Raf kinase inhibitor dabrafenib for the treatment of metastatic melanoma. However, introduction of the *tert*-butyl substituent is often accompanied by a substantial increase in logD and logP, which can lead to decreased aqueous solubility and increased rate of metabolism. Several bioisosteric replacements for the *tert*-butyl group have been proposed, many of which rely on fluorine substitution to reduce hydrophobicity and block undesired metabolism. [97] It is possible that these isosteric replacements could be beneficial for further development of the **PAC-1** derivatives described in this study.

3.8. Improving pharmacokinetics by removal of metabolic liabilities

3.8.1. Library design—One of the main challenges in using **PAC-1** in animals is the relatively short *in vivo* half-life (2.1 ± 0.3 h in dogs) [45] following i.v. administration. A study identified three main types of Phase 1 metabolism for **PAC-1** *in vivo*, including oxidative *N*-dealkylation, olefin oxidation, and arene oxidation (Figure 10). [98] Many of these metabolites still contain the *ortho*-hydroxy-*N*-acylhydrazone and therefore may be active, but the alcohols and secondary amines present in these metabolites can form conjugates including sulfates and glucuronides, which are then cleared from circulation. The metabolic liabilities present in **PAC-1** likely contribute to its rapid clearance. A **PAC-1** analogue that cannot be metabolized to the same extent may allow for therapeutic effects from doses at lower levels or lower frequency.

A library of 45 **PAC-1** analogues (**PAC-1**, **S-PAC-1**, **14a**, and **38–79**) was designed with the goal of enhancing metabolic stability (Figure 11). [50] The library was constructed by the condensation of nine hydrazides (**80a–i**) and five aldehydes (**81a–e**). To minimize oxidative *N*-dealkylation, building blocks containing a benzoyl group (**80c**, **80e**, **80g**, and **80i**) were introduced. Modifications to prevent oxidation of the olefin included removal of the allyl group (**81c**) or substitution with the fully saturated *n*-propyl group (**81b** and **81e**). Strategies to block arene oxidation included introduction of nitrile (**80d** and **80e**), fluorine (**80f**, **80g**, and **81c–e**), and trifluoromethyl (**80h** and **80i**) substituents.

3.8.2. Library evaluation—After synthesis was complete, the ability of the compounds to induce cell death in U-937 (human lymphoma) cells in culture was determined (Table 11). Each of the compounds was found to induce dose-dependent cell death under these conditions, and most of the compounds were approximately as potent as **PAC-1** and **S-PAC-1**, confirming the previously determined SAR. [15, 43, 44, 46] Following cell culture evaluation, the metabolic stability of the compounds was evaluated in rat liver microsomes after a 3 hour treatment at 10 μ M, and metabolites were observed by LC/MS (Table 11). The beta-adrenergic antagonist (\pm)-propranolol hydrochloride was included as a positive control; [99] under these conditions approximately 20% of the control remained. Compounds that contained benzoyl substituents were significantly more stable than analogous compounds containing benzyl groups; for example, compound **38** was more stable than **PAC-1**, and compound **66** was more stable than compound **65**. The propyl-containing compounds were less stable than the allyl-containing compounds (e.g., **PAC-1** was more stable than compound **44**), although the dihydroxylated metabolites were not observed for propyl-substituted compounds. In addition, **S-PAC-1** was relatively stable in the liver microsomes, despite the short *in vivo* half-life of the compound, [44] suggesting that clearance mechanisms other than oxidative metabolism play a greater role in the elimination of **S-PAC-1** from treated animals.

Selected compounds were then evaluated in mice (C57BL/6) to determine the tolerability (Table 11); compounds with improved tolerability would be considered for further evaluation. Compounds were formulated at 5 mg/mL in 200 mg/mL aqueous HP β CD (pH 5.5), and a dose of 200 mg/kg was administered to mice via i.p. injection (exceptions to this protocol are noted in Table 11). This dose of **PAC-1** induces severe but transient neuroexcitation; no adverse effects to **S-PAC-1** are observed at this dose. Responses to compounds were graded as mild, moderate, or severe; compounds that were lethal to the mice are also noted. Because of the high toxicity of compounds **43** and **52** and hemolysis induced by compound **70** *in vivo*, **PAC-1** derivatives containing the (trifluoromethyl)benzoyl substituent were not pursued beyond this evaluation.

3.8.3. Secondary biological assays—Four compounds (**41**, **64**, **66**, and **75**; structures in Table 12) were identified that were potent in cell culture, metabolically stable *in vitro* and well tolerated *in vivo*. In order to ascertain if the hit compounds induce cell death via similar mechanisms as **PAC-1**, the ability of compounds to chelate zinc *in vitro*, activate executioner caspases in whole cells, and induce apoptosis in cancer cells was evaluated. Zinc binding was determined using an EGTA titration experiment. [100] As shown in Table 12, **PAC-1** binds zinc with a K_d of 1.28 ± 0.03 nM, while **S-PAC-1** binds zinc with a K_d of 2.72 ± 0.13 nM. Each of the four new compounds displays affinity for zinc in the range of 1–2 nM, while inactive derivative **PAC-1a** does not bind zinc. [43]

In addition, the ability of compounds to activate executioner caspases in cell culture was evaluated. Cells were treated with compound for 0 or 16 hours, then the cells were lysed, and cleavage of the fluorescent caspase-3/-7 substrate Ac-DEVD-AFC was analyzed. As shown in Table 12, **PAC-1** induced nearly 90% caspase activation, while each of the other active compounds induced greater than 60% activation of the executioner caspases, relative

to the positive control compound staurosporine. As expected, treatment with DMSO alone or **PAC-1a** induced minimal caspase activity in the cells. [50]

In order to confirm that the compounds induced cell death via apoptosis, U-937 cells were treated with compounds at 50 μM for 12 hours, and cells were stained with Annexin V-FITC/propidium iodide and analyzed via flow cytometry (Figure 12). Each of the compounds induced approximately 50% cell death, and the large populations of Annexin V-FITC positive, propidium iodide negative cells demonstrates that the compounds induce apoptosis. [50]

Because many **PAC-1** derivatives induce cell death in white blood cell cancer lines [15, 24, 43, 44, 46, 48, 49, 52–55] and primary isolates from leukemia [23] and multiple myeloma patients [24] in culture, the cytotoxicity of the compounds in a series of lymphoma and leukemia cell lines, including Jurkat (human leukemia), GL-1 (dog lymphoma), OSW (dog lymphoma), and EL4 (mouse lymphoma) cells, in order to complement the previously determined IC_{50} values in U-937 (human lymphoma) cells. As shown in Table 13, comparable potency was observed across each given cell line. [50]

3.8.4. Pharmacokinetics—Based on their similar activity to **PAC-1** and **S-PAC-1** *in vitro* and in cell culture, the pharmacokinetics of compounds **41**, **64**, **66**, and **75** were evaluated in mice following an i.v. injection or oral gavage of 25 mg/kg and compared to **PAC-1** and **S-PAC-1** (Figure 13 and Table 14). Clearance of **PAC-1** and **S-PAC-1** from circulation was rapid, and detectable levels of the compounds were not present after 5 hours (**PAC-1**) or 6 hours (**S-PAC-1**) post-treatment. The four new derivatives had extended pharmacokinetic profiles, and compounds were detected in serum up to at least 8 hours post-treatment. [50]

PAC-1 had an elimination half-life of 24.6 ± 0.9 minutes, and **S-PAC-1** had an elimination half-life of 38.1 ± 3.3 minutes. The half-lives of the four new derivatives were at least three-fold higher than that of **PAC-1**, and AUC values from i.v. administration were all considerably higher as well. In addition, oral bioavailability of **41**, **66**, and **75** was higher than for **PAC-1** and **S-PAC-1**. [50]

3.9. Summary of libraries

To date, over 1000 **PAC-1** derivatives have been synthesized and evaluated. These derivatives have convincingly demonstrated the essential nature of the *ortho*-hydroxy-*N*-acylhydrazone on procaspase-3 activation and anticancer activity. The available data suggest that the ability of this motif to chelate labile inhibitory zinc away from cellular procaspase-3 is responsible for the induction of cell death; **PAC-1** chelates zinc within cells (as discussed in Section 4.4), [47] and modifications to the *ortho*-hydroxy-*N*-acylhydrazone lower the affinity for zinc and the cytotoxicity.[43, 60] Many of the most potent derivatives contained hydrophobic moieties, and it is likely that the hydrophobicity improves cell permeability. [46]

As a result of the library syntheses, four **PAC-1** derivatives were identified and selected for further evaluation. The library for SAR determination [43] facilitated the design of **S-PAC-1**, which was evaluated extensively in cell culture and in canine cancer patients. [44, 47]

WF-210 and **WF-208** emerged from the oxadiazole library, and the compounds were evaluated in cell culture and murine xenograft tumor models. [48, 49] Finally, **B-PAC-1** was synthesized as part of the 837-membered combinatorial library, [46] and the compound showed activity against primary isolates from leukemia patients, [23] as well as in cell lines and primary isolates from multiple myeloma patients [24] in culture. The remainder of this article describes the detailed evaluation of these four **PAC-1** derivatives.

4. S-PAC-1

4.1. Discovery and initial evaluation

Studies have shown that **PAC-1** can induce neuroexcitation *in vivo* at elevated doses when given via i.v. or i.p. injection. Seizures are observed after administration of high doses via i.v. or i.p. injection in animals, with lethality at very high doses. [44] It was hypothesized that in order to induce this neuroexcitation, **PAC-1** must cross the blood-brain barrier (BBB), although the specific interactions leading to this phenotype are not well understood. Therefore, in order to develop a compound with improved safety, the design of a **PAC-1** derivative that would not cross the BBB was explored. Compounds that cross the BBB tend to be small, rigid, and lipophilic; [101] therefore, the introduction of a polar substituent would help prevent passage of the compound across the BBB. With the knowledge that substituents on the aromatic rings of **PAC-1** could be modified while still maintaining anticancer activity, [43] a derivative containing a highly polar sulfonamide group, **S-PAC-1** (**37**, Table 10), was designed and developed by researchers in the Hergenrother group. **S-PAC-1** bound zinc with comparable affinity to that of **PAC-1**, and it was able to relieve zinc-mediated inhibition of procaspase-3 *in vitro*, although it was not as potent as **PAC-1** in this assay. [44]

After confirmation that **S-PAC-1** was active *in vitro*, **S-PAC-1** and **PAC-1** were evaluated in cell culture against a panel of cell lines over 72 hours (Table 15). In preparation for an animal model of lymphoma, five lymphoma cell lines were evaluated, including U-937 (human), EL4 (mouse), 17-71 (dog), GL-1 (dog), and OSW (dog). **PAC-1** and **S-PAC-1** both displayed IC₅₀ values in the low micromolar range for all five cell lines evaluated. The compounds were also evaluated in four additional human cancer cell lines, including Jurkat (leukemia), SK-MEL-5 (melanoma), HeLa (cervical), and MDA-MB-231 (breast), and comparable potency was observed across these cell lines as well. Investigation of the mode of cell death induced by **S-PAC-1** was performed by treatment of U-937 cells with **S-PAC-1** and staining with Annexin V-FITC/propidium iodide. Flow cytometry analysis indicated that **S-PAC-1** induces cell death via apoptosis. [44]

In order to determine an effective *in vivo* dosing regimen, the cytotoxicity of **S-PAC-1** was evaluated after varying treatment times (Table 16). U-937 cells were treated with **S-PAC-1** for times ranging from 1–72 hours. The compound was then washed out, and cells were allowed to grow until 72 hours after the initiation of treatment. The compound induces minimal cell death at time points up to 6 hours, and the first toxicity is observed at 9 hours. The potency increases until 24 hours and does not change significantly between 24–72

hours. These results indicated that in order to observe anticancer efficacy *in vivo*, serum concentrations of 10 μM for at least 24 hours would be most effective.[44]

4.2. Safety and pharmacokinetics

S-PAC-1 was advanced to *in vivo* experiments based on its promising activity *in vitro* and in cell culture. **S-PAC-1** was administered to mice via i.v. injection, and no adverse effects were observed at doses up to 350 mg/kg. In contrast, **PAC-1** induces mild neurological symptoms at doses as low as 20 mg/kg when administered via i.v. injection. The pharmacokinetic profiles of **PAC-1** and **S-PAC-1** were evaluated, and the peak plasma concentration was compared between **S-PAC-1** at 350 mg/kg and **PAC-1** at 20 mg/kg, the lowest dose to induce neurological symptoms, and 50 mg/kg, a dose at which neurotoxicity is severe. The maximum serum concentration of **PAC-1** at 20 mg/kg was approximately 50 μM , and the maximum concentration at 50 mg/kg was approximately 100 μM . However, the 350 mg/kg dose of **S-PAC-1** resulted in serum concentration of approximately 3500 μM , a 70-fold increase over the threshold for induction of neurotoxicity for **PAC-1**. [44]

Despite the improved safety profile of **S-PAC-1**, evaluation in murine tumor models was not practical due to the rapid clearance of the compound from circulation; the half-life was approximately 1 hour following IP administration of compound to mice (Figure 14A). Therefore, further *in vivo* evaluation of **S-PAC-1** was performed in dogs. A 25 mg/kg intravenous dose of **S-PAC-1** administered over 10 minutes (Figure 14B) was well tolerated and gave a peak plasma concentration of approximately 150 μM . However, the compound was cleared rapidly from dogs as well, with an elimination half-life of 1.09 ± 0.02 hours. In order to achieve serum concentrations of 10 μM for 24 hours, a continuous-rate infusion strategy was investigated, with an initial loading dose administered over 10 minutes, followed by a maintenance dose over 24 hours (Figure 14C). Healthy research dogs tolerated the continuous administration of **S-PAC-1** well, and a loading dose of 7 mg/kg followed by a constant-rate infusion of 3 mg/kg/h was chosen to achieve a serum concentration of 10 μM during the course of the treatment. [44]

4.3. Evaluation in canine lymphoma patients

With an understanding of the pharmacokinetics of **S-PAC-1** upon continuous-rate infusion in place, a clinical trial of six canine lymphoma patients was initiated. Three patients received four doses via 24-hour continuous infusions once weekly, while three additional patients received two 72-hour continuous infusions two weeks apart. In general, the 7 mg/kg loading dose followed by the 3 mg/kg/h continuous infusion was successful in maintaining the desired 10 μM serum concentration during the administration. No hematologic or nonhematologic toxicity was observed in any of the six patients, and only minor adverse events were reported, including mild gastrointestinal symptoms and localized irritation at the site of injection. Encouragingly, one of the six patients showed a partial response to **S-PAC-1** therapy (Figure 15). A 30% reduction in the tumor size was observed both by caliper RECIST score and CT scan of the lymph nodes. Three of the patients showed stable disease, while two showed disease progression. Flow cytometry analysis of lymph node aspirates from two patients demonstrated the presence of procaspase-3 prior to treatment, as well as an increase in cleaved caspase-3 seven days after initiation of treatment. An increase in the

tumor volume in all six patients was observed after therapy ceased, suggesting that the tumors reverted to their pre-treatment growth rate, and that dosing with increased amounts and/or frequency of treatment may be necessary for durable anticancer efficacy. These results provide the first validation for procaspase-3 activation as an anticancer strategy in spontaneous tumors. [44]

4.4. Comparison to PAC-1

Efforts were undertaken to further elucidate the mechanism of action of **PAC-1** and **S-PAC-1** in order to further understand the significant difference in tolerability. [47] An initial experiment involved treatment of HeLa cells containing the genetically encoded fluorescent zinc sensor ZapCY2. This sensor contains a zinc finger conjugated to cyan fluorescent protein (CFP) and yellow fluorescent protein (YFP). The sensor undergoes a conformational change upon binding to zinc, allowing for fluorescence resonance energy transfer (FRET) to occur between CFP and YFP, and the YFP fluorescence is observed. Release of zinc prevents FRET, and CFP fluorescence is observed. Therefore, the cellular zinc concentration is proportional to the FRET ratio (FRET/CFP). [102] Both **PAC-1** and **S-PAC-1** reduced intracellular zinc concentrations within seconds after addition of compound, and the rate and amount of zinc sequestration were similar for both compounds (Figure 16). These results provide the first demonstration that **PAC-1** and **S-PAC-1** bind the labile pool of zinc within cells. [47]

To confirm that the compounds act similarly in cells, a transcript profiling experiment was performed to assess differences in global gene expression upon treatment with compounds. In this experiment, HL-60 cells were treated with either **PAC-1** or **S-PAC-1** at 25 μM , mRNA was collected after six hours, and the transcript levels were compared to a vehicle-treated control. There was a very high correlation between the two different treatment groups; many of the most upregulated transcripts for **PAC-1** were also highly upregulated in **S-PAC-1**, while expression of many of the most downregulated transcripts for **PAC-1** was also suppressed for **S-PAC-1** treatment. The degree of similarity was measured by calculating the Spearman rank correlation value for the two treatment groups. The value was calculated at 0.928, very close to a perfect correlation of 1.0, demonstrating that **PAC-1** and **S-PAC-1** induce a similar transcriptional response and likely act similarly within cells at the 25 μM concentration. [47]

In order to further understand the difference in the observed neurological phenotypes for **PAC-1** and **S-PAC-1**, experiments were performed to determine the ability of the compounds to penetrate relevant physiological barriers (Figure 17). It was proposed that **PAC-1** enters the brain to induce the neuroexcitation by a mechanism that is not yet well understood, while the polar sulfonamide group prevents **S-PAC-1** from crossing the BBB. [44] An initial experiment demonstrated that equal concentrations of **PAC-1** and **S-PAC-1** enter Neuro-2a (murine neuroblastoma) cells after incubation with either compound at 50 μM for 30 minutes (Figure 17A), suggesting that the difference in toxicity is not related to a difference in cell permeability. Following this, an experiment was performed to determine the BBB permeability of the compounds *in vivo* (Figure 17B–C). C57BL/6 mice were administered **PAC-1** or **S-PAC-1** at 75 mg/kg via i.v. injection. Mice were sacrificed after

five minutes, samples from blood and brains were collected, and concentrations were analyzed by HPLC. **PAC-1** displayed approximately 30:70 distribution between brain and blood, consistent with the observed neurological phenotype. In contrast, less than 1% of **S-PAC-1** entered the brain. [47] This difference in BBB permeability is most likely sufficient to explain the difference in neuroexcitation, although further experiments on the mechanism of neuroexcitation are necessary to determine whether other factors may be partially responsible.

Finally, the effect of treatment time on cell death induced by **PAC-1** and **S-PAC-1** was assessed in order to determine effective dosing strategies for *in vivo* studies. U-937 cells were treated with compounds at 100 μM for 4, 8, 12, or 24 hours. The cells were then washed, and fresh growth medium was added. Cell death was assessed 24 hours after the initiation of treatment via Annexin V-FITC/propidium iodide staining. The results are shown in Figure 18. **PAC-1** induced greater than 50% cell death after only 4 hours, and greater than 90% of cells were no longer viable after an 8-hour treatment. In contrast, **S-PAC-1** induced apoptosis much more slowly; the 50% cell death threshold was reached between 8–12 hours of treatment. [47] This is consistent with the previous study on the rate of apoptosis induced by **S-PAC-1**. [44] Taken together, these results suggest that achieving a high serum concentration for a short time period may represent an effective dosing strategy for **PAC-1**, while serum concentrations of **S-PAC-1** should be higher for sustained periods of time in order to achieve efficacy.

5. WF-210 and WF-208

5.1. Discovery and initial evaluation

As discussed above, a series of oxadiazole-containing **PAC-1** derivatives were synthesized and evaluated in HL-60 cells in a 72-hour experiment by Gong, Wu, and coworkers. [48, 49] The two most potent compounds identified from this assay, with IC_{50} values of 80 nM, were **WF-208 (27r)** and **WF-210 (27s)**, each of which contains a piperonylthiazole attached to the benzylidene ring and a halogen-substituted (phenoxy)methylphenyl group attached to the oxadiazole (structures in Table 7). [48, 49]

PAC-1 and the two new derivatives were then evaluated in a panel of 15 human cancer cell lines in culture for their ability to induce cell death (Table 17). The cell lines represented a wide range of tumor types, including leukemia, lung cancer, liver cancer, gastric cancer, breast cancer, glioma, prostate cancer, colon cancer, and gallbladder cancer. In general, **WF-208** and **WF-210** were highly potent in the cell lines evaluated, with 72-hour IC_{50} values in the mid-nanomolar to low micromolar range, and potency was greater than that of **PAC-1** in all cell lines evaluated. In addition, all three compounds were evaluated in four non-cancerous cell lines. Less than 50% cell death was observed at concentrations up to 100 μM , suggesting the potential for selectivity of cancer cell death over healthy tissue toxicity *in vivo*. [48, 49]

5.2. Caspase-dependent cell death

The dependence of caspase activity on cell death induced by **PAC-1**, **WF-208**, and **WF-210** was evaluated in a detailed series of assays. The first set of experiments demonstrated the ability of the compounds to activate caspase enzymes in cells. Treatment of HL-60 or U-937 cells with **PAC-1**, **WF-208**, or **WF-210** for time periods between 0 and 24 hours, followed by immunofluorescence staining for cleaved caspase-3, indicated that each compound led to the activation of caspase-3 in a dose- and time-dependent manner. The cells were then treated with **PAC-1** (50 μ M), **WF-208** (10 μ M), or **WF-210** (10 μ M), and western blotting was used to analyze procaspases-3, -8, and -9, as well as poly (ADP-ribose) polymerase (PARP), a canonical caspase-3 substrate (Figure 19). For each compound in both cell lines, cleavage of procaspase-3 and PARP were the earliest events, followed by cleavage of procaspases-8 and -9. These results were further supported by analysis of fluorogenic substrates for each of these three caspase enzymes. In HL-60 cells treated with **PAC-1** or **WF-210**, caspase-3 activity was detected as early as 1 hour after the initiation of treatment, followed by caspase-8 and -9 activities at 4 hours. In contrast, cells treated with the DNA topoisomerase II inhibitor etoposide, which induces apoptosis via the intrinsic pathway, showed caspase-3 and -9 activities simultaneously at 4 hours, followed by caspase-8 at 6 hours. These results suggest that **PAC-1** and derivatives induce apoptosis via a different mechanism than the canonical intrinsic or extrinsic pathways, and the observation that procaspase-3 is activated hours before procaspase-8 or -9 strongly supports the direct procaspase-3 activation mode of action for **PAC-1** and derivatives. [48, 49]

Following this experiment, HL-60 and U-937 cells were treated with compound for 12 hours (**WF-208**) or 24 hours (**PAC-1** and **WF-210**). Flow cytometry analysis with Annexin V-FITC/propidium iodide staining indicated significant portions of apoptotic cells. **WF-210** was more potent than **PAC-1** in this assay, while both compounds induced apoptosis to a greater degree after 24 hours than did **WF-208** at 12 hours. [48, 49]

The ability of caspase inhibitors to protect against apoptosis induced by **PAC-1** and derivatives was then evaluated. HL-60 and U-937 cells were treated for 24 hours with **PAC-1** (50 μ M), **WF-208** (10 μ M), or **WF-210** (10 μ M) alone or in combination with a pan-caspase inhibitor (Z-VAD-fmk), a caspase-3/-7 inhibitor (Z-DEVD-fmk), a caspase-8 inhibitor (Z-IETD-fmk), or a caspase-9 inhibitor (Z-LEHD-fmk). Cell death was assessed by Annexin V-FITC/propidium iodide staining. Apoptosis induced by all three compounds was significantly reduced by either the pan-caspase inhibitor or the caspase-3/-7 inhibitor, but not by the inhibitors of the initiator caspases. [48, 49] In addition, co-treatment of **WF-208** with zinc led to a decrease in cell death; [49] although this experiment was not performed with **WF-210**, previous experiments have shown the protective effects of zinc on apoptosis induced by **PAC-1** [42] and its derivative **B-PAC-1**. [23, 24]

Finally, the dependence on procaspase-3 for the cytotoxic activity of **PAC-1** and derivatives was studied using HL-60 cells, which overexpress procaspase-3, and MCF-7 (human breast cancer) cells, which do not express procaspase-3. Knockdown of caspase-3 in HL-60 cells with siRNA resulted in a loss of potency for all three compounds compared to a control siRNA. [48, 49] Further, the addition of a plasmid coding for procaspase-3 increased

susceptibility of MCF-7 cells to the **PAC-1** derivatives compared to the control plasmid; similar results with an analogous MCF-7 isogenic cell line pair has been observed by others with **PAC-1**. [56] Western blots for caspase-3 and PARP-1 demonstrated decreased procaspase-3 activation in knockdown HL-60 cells, as well as increased caspase-3 activity in transfected MCF-7 cells. In contrast, knockdown or overexpression of procaspase-3 showed no effect on the cytotoxicity of the pan-kinase inhibitor staurosporine or etoposide. These results support the importance of caspase-3 activity for the cytotoxicity of **PAC-1** and derivatives. [48, 49]

5.3. Antitumor efficacy *in vivo*

Based on favorable results from cell culture experiments, **PAC-1**, **WF-208**, and **WF-210** were evaluated in a series of murine xenograft tumor models. **PAC-1** and **WF-210** were first evaluated in Hep 3B (human hepatocellular carcinoma) and MDA-MB-435S (a human melanoma cell line, although erroneously described previously as a breast cancer cell line [103]) models. Mice received **PAC-1** (5 mg/kg) or **WF-210** (2.5 mg/kg) daily for two weeks via i.v. injection. Both compounds reduced tumor volume significantly compared to control in both models, although **WF-210** showed a greater effect than **PAC-1**, especially in the Hep 3B model and the MDA-MB-435S model. These results correlate with the increased cell culture potency of **WF-210** as compared with **PAC-1**. Western blots of samples derived from the tumors showed increased cleavage of caspase-3 and PARP-1 in both treatment groups compared to control. In addition, **WF-210** was evaluated in a GBC-SD (human gallbladder carcinoma) xenograft and a second MDA-MB-435S xenograft, with oral administration of compound (100 mg/kg). **WF-210** significantly reduced tumor volume compared to control in these models as well. Finally, **PAC-1** and **WF-210** were evaluated in an MCF-7 xenograft model. Since this cell line lacks functional procaspase-3, any efficacy in this model would suggest that factors other than procaspase-3 activation are important in **PAC-1** activity. Neither **PAC-1** (5 mg/kg i.v.) nor **WF-210** (2.5 mg/kg i.v.) demonstrated anticancer efficacy in the MCF-7 model, and western blots showed minimal PARP-1 cleavage in all treatment groups, again suggesting the importance of procaspase-3 for the mechanism of action of **PAC-1** and derivatives. [48]

PAC-1 and **WF-208** were evaluated in a PC-3 (human prostate cancer) model. Both compounds were given at 2.5 mg/kg via i.v. injection daily for 15 days. **WF-208** showed significant tumor reduction compared to control, while **PAC-1** showed no significant tumor reduction. Western blots of samples derived from the tumors demonstrated increased caspase-3 cleavage in samples from mice treated with **WF-208** or **PAC-1**, as well as increased PARP cleavage in **WF-208**-treated animals, further demonstrating the importance of procaspase-3 for **PAC-1** and **WF-208** activity. [49]

6. B-PAC-1

6.1. Discovery and cell death induction

From the combinatorial library discussed in Section 3.7, six highly potent **PAC-1** derivatives were discovered to induce apoptosis in U-937 cells. [46] One compound discovered from this library, named **B-PAC-1** (**36**{ 18, 7}, Table 10) for the benzyloxy and butyl substituents,

was evaluated by Gandhi and coworkers in patient-derived samples from chronic lymphocytic leukemia (CLL), [23] as well as in primary isolates and cell lines derived from multiple myeloma (MM) patients. [24]

B-PAC-1 induced apoptosis in CLL cells in a dose-dependent manner. Apoptosis was rapid; at 10 μM **B-PAC-1**, cells began to die as early as 6 hours post-treatment, and cell death was significant at 10 hours. Treatment of CLL lymphocytes across 38 samples with 10 μM **B-PAC-1** led to a median of 60% cell death. This was significantly greater than cytotoxicity to noncancerous peripheral blood mononuclear cells (median 21%, $n = 6$) or normal B lymphocytes (median 31%, $n = 6$), demonstrating potential selectivity for apoptosis induction by **B-PAC-1** in cancer cells over healthy cells. [23]

B-PAC-1 also induced apoptosis in MM cell lines. In both the MM.1S cell line and the U266 cell line, **B-PAC-1** induced dose-dependent cell death in a 24-hour experiment, and the degree of apoptotic cells increased with increasing treatment time. **B-PAC-1** was more potent than **PAC-1** in this experiment, while **PAC-1a** induced minimal cell death above the untreated controls. [24]

Current treatment for MM involves chemotherapy regimens that include dexamethasone, lenalidomide, and/or bortezomib, but resistance to these agents remains a challenge in the management of this disease. Therefore, the development of a novel agent that overcomes many of these mechanisms of resistance would represent a significant advance. Toward this goal, **B-PAC-1** was evaluated in MM cell lines that are sensitive to all three agents (MM.1S and KAS-6/1) or resistant to lenalidomide (MM1/R10R and KAS6/R10R), dexamethasone (MM.1R), or bortezomib (KAS-6/V10R). After 24 hours of treatment, **B-PAC-1** induced apoptosis in all six of these cell lines, and less than 20% cell viability was observed for all cell lines at 10 μM **B-PAC-1**. The compound induced similar responses between MM.1S and MM.1/R10R (Pearson correlation = 0.9806, $p = 0.0032$), and between MM.1S and MM.1R (Pearson correlation = 0.9778, $p = 0.004$). Similar responses were also observed between KAS-6/1 and KAS-6/R10R (Pearson correlation = 0.9978, $p = 0.0001$) and between KAS-6/1 and KAS-6/V10R (Pearson correlation = 0.9814, $p = 0.003$). [24]

In addition to the MM cell lines, **B-PAC-1** was evaluated in 11 primary isolates from MM patients. CD138+ myeloma cells were isolated from bone marrow aspirates of MM patients and treated with 0 or 20 μM **B-PAC-1** for 72 hours. Of the 11 samples, nine showed an increase in the percentage of apoptotic cells upon treatment with **B-PAC-1**, further demonstrating the promise of this agent. [24]

6.2. Role of zinc in B-PAC-1 activity

Because the proposed mechanism of action of **PAC-1** involves chelation of labile zinc, [42] experiments were performed to assess the role of zinc in **B-PAC-1** cytotoxicity. CLL cells were treated for 24 hours with the Bcl-2 inhibitor **ABT-199** (1 nM), staurosporine (100 nM), **B-PAC-1** (10 μM), or the negative control compound **PAC-1a** (10 μM), in the presence or absence of ZnSO_4 (100 μM). **ABT-199** and staurosporine induce apoptosis via the intrinsic pathway through mechanisms independent of zinc, while **PAC-1a** does not bind zinc. The addition of zinc fully inhibited cell death induced by **B-PAC-1**, consistent with the proposed

mechanism of action, while having no effect on the cytotoxicity of **ABT-199** or staurosporine. Treatment with **PAC-1a** or ZnSO₄ alone did not induce apoptosis. Similar results were observed whether zinc was added at the same time as **B-PAC-1** or five hours later, and zinc protected against **B-PAC-1** cytotoxicity in a dose-dependent manner. [23]

The addition of zinc was also protective against apoptosis induced by **B-PAC-1** in MM cells. At 3 and 10 μM, **B-PAC-1** decreased the viability of MM.1S cells during a 24-hour treatment. However, the addition of 100 μM ZnSO₄ restored cell viability to control levels; cell viability after treatment with ZnSO₄ alone was also comparable to untreated levels. Cells were also susceptible to staurosporine (100 nM), and the addition of ZnSO₄ did not abolish the cytotoxicity of this agent, suggesting a distinct mechanism of action for **B-PAC-1** compared to other proapoptotic agents. [24]

For the development of any therapeutic metal-chelating compound, it is important to ensure that chelation will be selective for the metal ion of interest, in order to minimize off-target effects. For this reason, **B-PAC-1** was evaluated *in vitro* against carboxypeptidase A and histone deacetylase, two zinc-dependent enzymes. **B-PAC-1** showed no inhibition of either enzyme, confirming the selectivity of **PAC-1** derivatives for sequestration of labile zinc over essential metal ions. [23]

6.3. Role of apoptotic proteins in **B-PAC-1** activity

Several experiments were performed in order to assess the role of caspase activity in **B-PAC-1**-mediated apoptosis. After 24 hours of treatment with **B-PAC-1** (10 μM), increased cleavage of initiator caspases-8 and -9, as well as executioner caspases-3 and -7 was observed by western blot; executioner caspase-6 was not activated in response to **B-PAC-1** treatment. In addition, the caspase-3 substrate PARP-1 was cleaved in the treated samples, but not in untreated samples, demonstrating that **B-PAC-1** induces caspase-3 activation in CLL cells. [23]

B-PAC-1 also induced activation of executioner caspases-3, -6, and -7 in MM cells. A 24 hour treatment with **B-PAC-1** (5 or 10 μM) resulted in decreased levels of procaspases-3, -6, and -7, as observed by western blot, as well as increased levels of cleaved caspases-3 and -7. Cleaved caspase-6 was not detected, likely due to lower expression and/or rapid degradation of the enzyme. The addition of 100 μM ZnSO₄ inhibited the cleavage of the executioner caspases. Procaspase-3 cleavage was also observed after treatment with staurosporine (100 nM), and the addition of zinc had minimal effect on the disappearance of procaspase-3. [24]

Following these experiments, the effect of genetic knockdown of key apoptotic proteins on **B-PAC-1** activity was evaluated. The extent of apoptosis induced by **B-PAC-1** (5 μM) or staurosporine (100 nM) in wild-type Jurkat cells was identical to the cell death in caspase-8 double knockout Jurkat cells (Casp8 (-/-)) in a 24-hour treatment. In contrast, the Fas ligand (100 ng/mL), which induces apoptosis via the extrinsic pathway, was cytotoxic in wild-type Jurkat cells but showed minimal cytotoxicity in Casp8 (-/-) cells. These results suggest that the extrinsic pathway is not important in **B-PAC-1** cytotoxicity, and that caspase-8 is most likely cleaved after the activation of caspase-3 or -7. [23]

The role of caspases-3 and -7 in **B-PAC-1** activity was then evaluated, using mouse embryonic fibroblasts (MEFs) with a single knockout of both genes (Casp3/7 (+/-)) or a double knockout of both genes (Casp3/7 (-/-)), and cells were treated with compounds for 24 hours. Both staurosporine (100 nM) and **B-PAC-1** (5 μ M) were equally potent in the wild-type and Casp3/7 (+/-) MEFs, but a significant decrease in cell death was observed for each compound in the Casp3/7 (-/-) MEFs. These results demonstrate the importance of the executioner caspases in **B-PAC-1** activity. [23]

In addition, the role of proapoptotic Bcl-2 family proteins Bax and Bak in **B-PAC-1**-mediated apoptosis was evaluated. Both proteins were doubly knocked down in MEFs (Bax/Bak (-/-)), and the cells were treated with staurosporine (100 nM) or **B-PAC-1** (2 or 5 μ M) for 24 hours. **B-PAC-1** was not cytotoxic at 2 μ M, but approximately 50% cell death was observed in both the wild-type and Bax/Bak (-/-) MEFs at 5 μ M **B-PAC-1**. In contrast, staurosporine induced nearly 100% cell death in wild-type MEFs, but minimal cell death was observed in Bax/Bak (-/-) MEFs. [23]

The effect of increased expression of antiapoptotic Bcl-2 family proteins Bcl-2, Bcl-X_L, and Mcl-1 was also investigated. HL-60 cells were transfected with Bcl-2 (HL-60/Bcl-2), Bcl-X_L (HL-60/Bcl-X_L), or a control vector (HL-60/Neo), and each of these three cell lines was treated with **B-PAC-1**. Dose-dependent cell death in response to **B-PAC-1** was observed at similar levels for all three cell lines. In a second experiment, MEFs containing intact Mcl-1 or with a genetic deletion (Mcl-1^{-/-}) were treated with **B-PAC-1**. In both the wild-type and Mcl-1^{-/-} cells, **B-PAC-1** induced dose-dependent cell death to a similar extent. [24] These results indicate that **B-PAC-1** can induce apoptosis independent of certain upstream apoptotic effector proteins.

Finally, the ability of pan-caspase inhibitors Z-VAD-fmk and Q-VD-OPh to inhibit **B-PAC-1**-induced apoptosis was assessed. In a 24-hour experiment, Z-VAD-fmk and Q-VD-OPh (50 μ M each) partially but significantly reduced the extent of apoptosis induced by **B-PAC-1** (10 μ M); both fully inhibited apoptosis induced by staurosporine (100 nM). In addition, the effect of these inhibitors on PARP-1 cleavage was assessed by western blot. Co-treatment of **B-PAC-1** (10 μ M) or **ABT-199** (5 nM) with Q-VD-OPh (50 μ M) fully inhibited cleavage of PARP-1, while co-treatment with Z-VAD-fmk (50 μ M) partially reduced the amount of cleaved PARP-1 detected. [23] Combined, these results from the Gandhi laboratory strongly support a direct procaspase-3 activation mode of action for **B-PAC-1**.

6.4. Combination of **B-PAC-1** with a Smac mimetic

Smac, a proapoptotic protein, binds to the antiapoptotic IAPs and inhibits their interactions with caspase-3 (Figure 1). This relief of inhibition allows for caspase-3 to cleave its substrates, and cells undergo apoptosis. [1] Many small-molecule mimics of Smac, including **SM-164**, [13] **LCL-161**, [14] and **Smac066**, [104] are currently under investigation as anticancer agents. Treatment of CLL cells with **B-PAC-1** led to an elevation in Smac protein levels. Because this effect was observed, it was proposed that a small molecule with Smac-like activity could synergize with **B-PAC-1** to induce apoptosis. Cells were treated with **B-**

PAC-1, **Smac066**, or a combination at 5, 7.5, or 10 μM . Combinations were synergistic for the majority of samples evaluated, as measured by combination indices of less than 1.0, demonstrating the potential for induction of apoptosis via combination therapy with **B-PAC-1** and additional proapoptotic agents. [23]

7. SUMMARY AND OUTLOOK

In March 2015, a Phase 1 clinical trial of **PAC-1** in human cancer patients was initiated (NCT02355535); the activation of procaspase-3 by small molecules appears to be a promising anticancer strategy. Because procaspase-3 is elevated in a variety of different tumor types, induction of apoptosis via the removal of labile inhibitory zinc from procaspase-3 has the potential to treat a diverse array of tumors, both as single agent drugs and in combination with other anticancer agents. The efficacy of **PAC-1** and related derivatives in cell culture and in the *in vivo* cancer models reinforce the hypotheses formed from *in vitro* data, and has led to the Phase 1 clinical trial.

PAC-1 has been studied extensively; cell culture and *in vivo* anticancer efficacy have been promising, [15] and the initial efficacy studies combined with the demonstrated BBB permeability [47] suggest the potential for the treatment of CNS cancers. [105] Rapid clearance from circulation in mice [45] necessitates the administration of relatively large doses to these animals, and the observed neuroexcitation [44] may prove dose-limiting. In this regard, human pharmacokinetic data will be very informative and crucial for the further advancement of **PAC-1**. Prudence suggests that drugs should not be CNS penetrant unless necessary; thus, there is considerable value in the development of non-BBB penetrant **PAC-1** derivatives for the treatment of non-CNS tumors. With the goal of identifying a BBB-impermeable **PAC-1** derivative, **S-PAC-1**, containing a highly polar sulfonamide group, was designed. [44] *In vivo* evaluation demonstrated that the sulfonamide successfully prevented entry into the brain, [47] and the compound showed promise in a clinical trial in canine lymphoma patients. [44] **S-PAC-1** is also rapidly cleared from mice and dogs, which required a continuous infusion strategy for administration to patients. [44] It is possible that favorable pharmacokinetics may be achieved via oral administration, although this has not yet been reported on.

Gong, Wu, and coworkers identified **WF-208** and **WF-210** as highly potent **PAC-1** derivatives in cell culture across a wide variety of cell lines, and with considerably greater potency in cancer cells compared to non-cancerous cell lines. Extensive studies of **PAC-1** and these two derivatives demonstrated the necessity for procaspase-3 on the mechanism of action and showed that apoptosis occurs independent of upstream events, with procaspase-3 activation prior to cleavage of initiator procaspases-8 or -9. Both compounds showed anticancer efficacy in various mouse xenograft models, and both were reported to be well tolerated by mice. [48, 49] The initial studies demonstrate the promise for these two compounds as anticancer agents. The compounds are both much larger than typical small molecule drugs, with molecular weights of approximately 800, although **WF-210** demonstrated efficacy in two tumor models upon oral administration. It is possible that the bioavailability will be acceptable, although the compound appears to show improved efficacy upon i.v. injection as compared to oral administration. If the size of these

compounds prevents them from advancing further, it will be useful to determine the structural features responsible for the improved activity, to determine if any portion of the molecules can be removed without a loss in potency. In addition, it is unknown whether these compounds are BBB permeable, but given the large compound sizes, it is unlikely that high concentrations of these compounds are present in the brains of treated animals.

Six highly potent **PAC-1** derivatives were identified from the library of 837 compounds discussed in Section 3.7, [46] and **B-PAC-1** was selected for further evaluation. [23, 24] **B-PAC-1** was cytotoxic to primary isolates from leukemia patients in culture, and cytotoxicity was higher for cancer cells than healthy cells. **B-PAC-1** also induced apoptosis in primary isolates and cell lines derived from multiple myeloma patients. Studies on the mechanism of action demonstrated the necessity for procaspase-3 and zinc, as well as the non-canonical apoptotic pathway that was observed for **PAC-1**, **WF-208**, and **WF-210**. [23] Initial results from the **PAC-1** derivatives discussed above have demonstrated therapeutic potential, although challenges exist for all of the compounds. To date, **PAC-1** is the most promising compound for CNS tumors, and therapeutically relevant doses can be administered safely to animals. The most likely application for the other compounds discussed, including **S-PAC-1**, **WF-208**, **WF-210**, and **B-PAC-1**, would be tumors not present in the CNS. **S-PAC-1** was evaluated in canine lymphoma patients with promising initial results. **B-PAC-1** is cytotoxic to cells derived from white blood cell cancers in culture; *in vivo* efficacy has not yet been reported. **WF-208** and **WF-210** have demonstrated cytotoxicity in a wide variety of cancer cell lines in culture and have shown anticancer efficacy in several murine tumor models, although the large size of these compounds may complicate their translation to the clinic. Further evaluation of these and other agents will help to fully define the ability of procaspase activators to treat diverse cancers.

Acknowledgments

We are grateful to the National Institutes of Health (Grant R01-CA120439) and University of Illinois for support of this work. H.S.R. was partially supported by the Richard B. Silverman Predoctoral Fellowship from the American Chemical Society Division of Medicinal Chemistry. We thank Dr. Quinn P. Peterson for assistance with the creation of Figure 1.

Abbreviations used

PAC-1	procaspase-activating compound 1
SAR	structure-activity relationships
AUC	area under the concentration-time curve
i.v	intravenous
i.p	intraperitoneal
CLL	chronic lymphocytic leukemia
MM	multiple myeloma

References

1. Hengartner MO. The biochemistry of apoptosis. *Nature*. 2000; 407(6805):770–776. [PubMed: 11048727]
2. Elmore S. Apoptosis: A review of programmed cell death. *Toxicol Pathol*. 2007; 35(4):495–516. [PubMed: 17562483]
3. Nicholson DW. Caspase structure, proteolytic substrates, and function during apoptotic cell death. *Cell Death Differ*. 1999; 6(11):1028–1042. [PubMed: 10578171]
4. Earnshaw WC, Martins LM, Kaufmann SH. Mammalian caspases: Structure, activation, substrates, and functions during apoptosis. *Annual Review of Biochemistry*. 1999; 68:383–424.
5. Slee EA, Adrain C, Martin SJ. Executioner caspase-3, -6, and -7 perform distinct, non-redundant roles during the demolition phase of apoptosis. *J Biol Chem*. 2001; 276(10):7320–7326. [PubMed: 11058599]
6. Sakahira H, Enari M, Nagata S. Cleavage of CAD inhibitor in CAD activation and DNA degradation during apoptosis. *Nature*. 1998; 391(6662):96–99. [PubMed: 9422513]
7. Hanahan D, Weinberg RA. The hallmarks of cancer. *Cell*. 2000; 100(1):57–70. [PubMed: 10647931]
8. Hanahan D, Weinberg RA. Hallmarks of cancer: the next generation. *Cell*. 2011; 144(5):646–674. [PubMed: 21376230]
9. Vassilev LT, Vu BT, Graves B, Carvajal D, Podlaski F, Filipovic Z, Kong N, Kammlott U, Lukacs C, Klein C, Fotouhi N, Liu EA. In vivo activation of the p53 pathway by small-molecule antagonists of MDM2. *Science*. 2004; 303(5659):844–848. [PubMed: 14704432]
10. Vu B, Wovkulich P, Pizzolato G, Lovey A, Ding Q, Jiang N, Liu JJ, Zhao C, Glenn K, Wen Y, Tovar C, Packman K, Vassilev L, Graves B. Discovery of RG7112: A small-molecule MDM2 inhibitor in clinical development. *ACS Med Chem Lett*. 2013; 4(5):466–469. [PubMed: 24900694]
11. Oltersdorf T, Elmore SW, Shoemaker AR, Armstrong RC, Augeri DJ, Belli BA, Bruncko M, Deckwerth TL, Dinges J, Hajduk PJ, Joseph MK, Kitada S, Korsmeyer SJ, Kunzer AR, Letai A, Li C, Mitten MJ, Nettekheim DG, Ng S, Nimmer PM, O'Connor JM, Oleksijew A, Petros AM, Reed JC, Shen W, Tahir SK, Thompson CB, Tomaselli KJ, Wang BL, Wendt MD, Zhang HC, Fesik SW, Rosenberg SH. An inhibitor of Bcl-2 family proteins induces regression of solid tumours. *Nature*. 2005; 435(7042):677–681. [PubMed: 15902208]
12. Souers AJ, Levenson JD, Boghaert ER, Ackler SL, Catron ND, Chen J, Dayton BD, Ding H, Enschede SH, Fairbrother WJ, Huang DC, Hymowitz SG, Jin S, Khaw SL, Kovar PJ, Lam LT, Lee J, Maecker HL, Marsh KC, Mason KD, Mitten MJ, Nimmer PM, Oleksijew A, Park CH, Park CM, Phillips DC, Roberts AW, Sampath D, Seymour JF, Smith ML, Sullivan GM, Tahir SK, Tse C, Wendt MD, Xiao Y, Xue JC, Zhang H, Humerickhouse RA, Rosenberg SH, Elmore SW. ABT-199, a potent and selective BCL-2 inhibitor, achieves antitumor activity while sparing platelets. *Nat Med*. 2013; 19(2):202–208. [PubMed: 23291630]
13. Lu J, Bai L, Sun H, Nikolovska-Coleska Z, McEachern D, Qiu S, Miller RS, Yi H, Shangary S, Sun Y, Meagher JL, Stuckey JA, Wang S. SM-164: a novel, bivalent Smac mimetic that induces apoptosis and tumor regression by concurrent removal of the blockade of cIAP-1/2 and XIAP. *Cancer Res*. 2008; 68(22):9384–9393. [PubMed: 19010913]
14. Houghton PJ, Kang MH, Reynolds CP, Morton CL, Kolb EA, Gorlick R, Keir ST, Carol H, Lock R, Maris JM, Billups CA, Smith MA. Initial testing (stage 1) of LCL161, a SMAC mimetic, by the pediatric preclinical testing program. *Pediatr Blood Cancer*. 2012; 58(4):636–639. [PubMed: 21681929]
15. Putt KS, Chen GW, Pearson JM, Sandhorst JS, Hoagland MS, Kwon JT, Hwang SK, Jin H, Churchwell MI, Cho MH, Doerge DR, Helferich WG, Hergenrother PJ. Small-molecule activation of procaspase-3 to caspase-3 as a personalized anticancer strategy. *Nat Chem Biol*. 2006; 2(10):543–550. [PubMed: 16936720]
16. Wolan DW, Zorn JA, Gray DC, Wells JA. Small-molecule activators of a proenzyme. *Science*. 2009; 326(5954):853–858. [PubMed: 19892984]
17. Schipper JL, MacKenzie SH, Sharma A, Clark AC. A bifunctional allosteric site in the dimer interface of procaspase-3. *Biophys Chem*. 2011; 159(1):100–109. [PubMed: 21645959]

18. Vickers CJ, Gonzalez-Paez GE, Umotoy JC, Cayanan-Garrett C, Brown SJ, Wolan DW. Small-molecule procaspase activators identified using fluorescence polarization. *ChemBioChem*. 2013; 14(12):1419–1422. [PubMed: 23836614]
19. Ghavami S, Hashemi M, Ande SR, Yeganeh B, Xiao W, Eshraghi M, Bus CJ, Kadkhoda K, Wiechec E, Halayko AJ, Los M. Apoptosis and cancer: mutations within caspase genes. *J Med Genet*. 2009; 46(8):497–510. [PubMed: 19505876]
20. Soini Y, Paakko P. Apoptosis and expression of caspases 3, 6 and 8 in malignant non-Hodgkin's lymphomas. *APMIS*. 1999; 107(11):1043–1050. [PubMed: 10598877]
21. Wrobel G, Maldyk J, Kazanowska B, Rapala M, Maciejka-Kapuscinska L, Chaber R. Immunohistochemical expression of procaspase-3 and its clinical significance in childhood non-Hodgkin lymphomas. *Pediatr Dev Pathol*. 2011; 14(3):173–9. [PubMed: 20722551]
22. Estrov Z, Thall PF, Talpaz M, Estey EH, Kantarjian HM, Andreeff M, Harris D, Van Q, Walterscheid M, Kornblau SM. Caspase 2 and caspase 3 protein levels as predictors of survival in acute myelogenous leukemia. *Blood*. 1998; 92(9):3090–3097. [PubMed: 9787143]
23. Patel V, Balakrishnan K, Keating MJ, Wierda WG, Gandhi V. Expression of executioner procaspases and their activation by a procaspase activating compound in chronic lymphocytic leukemia cells. *Blood*. 2015; 125(7):1126–1136. [PubMed: 25538042]
24. Zaman S, Wang R, Gandhi V. Targeting executioner procaspase-3 with the procaspase activating compound B-PAC-1 induces apoptosis in multiple myeloma cells. *Exp Hematol*. 2015; 43(11):951–962. [PubMed: 26257207]
25. Fink D, Schlagbauer-Wadl H, Selzer E, Lucas T, Wolff K, Pehamberger H, Eichler HG, Jansen B. Elevated procaspase levels in human melanoma. *Melanoma Res*. 2001; 11(4):385–393. [PubMed: 11479427]
26. Chen N, Gong J, Chen X, Meng W, Huang Y, Zhao F, Wang L, Zhou Q. Caspases and inhibitor of apoptosis proteins in cutaneous and mucosal melanoma: expression profile and clinicopathologic significance. *Hum Pathol*. 2009; 40(7):950–956. [PubMed: 19269012]
27. Gdynia G, Grund K, Eckert A, Bock BC, Funke B, Macher-Goeppinger S, Sieber S, Herold-Mende C, Wiestler B, Wiestler OD, Roth W. Basal caspase activity promotes migration and invasiveness in glioblastoma cells. *Mol Cancer Res*. 2007; 5(12):1232–40. [PubMed: 18171980]
28. Murphy AC, Weyhenmeyer B, Schmid J, Kilbride SM, Rehm M, Huber HJ, Senft C, Weissenberger J, Seifert V, Dunst M, Mittelbronn M, Kogel D, Prehn JH, Murphy BM. Activation of executioner caspases is a predictor of progression-free survival in glioblastoma patients: a systems medicine approach. *Cell Death Dis*. 2013; 4:e629. [PubMed: 23681224]
29. Virkajarvi N, Paakko P, Soini Y. Apoptotic index and apoptosis influencing proteins bcl-2, mcl-1, bax and caspases 3, 6 and 8 in pancreatic carcinoma. *Histopathology*. 1998; 33(5):432–439. [PubMed: 9839167]
30. Persad R, Liu C, Wu TT, Houlihan PS, Hamilton SR, Diehl AM, Rashid A. Overexpression of caspase-3 in hepatocellular carcinomas. *Mod Pathol*. 2004; 17(7):861–867. [PubMed: 15098015]
31. Tormanen-Napankangas U, Soini Y, Kahlos K, Kinnula V, Paakko P. Expression of caspases-3, -6 and -8 and their relation to apoptosis in non-small cell lung carcinoma. *Int J Cancer*. 2001; 93(2):192–198. [PubMed: 11410865]
32. Krepela E, Prochazka J, Liul X, Fiala P, Kinkor Z. Increased expression of Apaf-1 and procaspase-3 and the functionality of intrinsic apoptosis apparatus in non-small cell lung carcinoma. *Biol Chem*. 2004; 385(2):153–168. [PubMed: 15101558]
33. Krepela E, Prochazka J, Fiala P, Zatloukal P, Selinger P. Expression of apoptosome pathway-related transcripts in non-small cell lung cancer. *J Cancer Res Clin Oncol*. 2006; 132(1):57–68. [PubMed: 16231180]
34. O'Donovan N, Crown J, Stunell H, Hill AD, McDermott E, O'Higgins N, Duffy MJ. Caspase 3 in breast cancer. *Clin Cancer Res*. 2003; 9(2):738–742. [PubMed: 12576443]
35. Zapata JM, Krajewska M, Krajewski S, Huang RP, Takayama S, Wang HG, Adamson E, Reed JC. Expression of multiple apoptosis-regulatory genes in human breast cancer cell lines and primary tumors. *Breast Cancer Res Treat*. 1998; 47(2):129–140. [PubMed: 9497101]

36. Krajewski S, Krajewska M, Turner BC, Pratt C, Howard B, Zapata JM, Frenkel V, Robertson S, Ionov Y, Yamamoto H, Perucho M, Takayama S, Reed JC. Prognostic significance of apoptosis regulators in breast cancer. *Endocr Relat Cancer*. 1999; 6(1):29–40. [PubMed: 10732784]
37. Nakopoulou L, Alexandrou P, Stefanaki K, Panayotopoulou E, Lazaris AC, Davaris PS. Immunohistochemical expression of caspase-3 as an adverse indicator of the clinical outcome in human breast cancer. *Pathobiology*. 2001; 69(5):266–273. [PubMed: 12107344]
38. Jiang H, Gong M, Cui Y, Ma K, Chang D, Wang TY. Upregulation of caspase-3 expression in esophageal cancer correlates with favorable prognosis: an immunohistochemical study from a high incidence area in northern China. *Dis Esophagus*. 2010; 23(6):487–492. [PubMed: 20113321]
39. Roy S, Bayly CI, Gareau Y, Houtzager VM, Kargman S, Keen SL, Rowland K, Seiden IM, Thornberry NA, Nicholson DW. Maintenance of caspase-3 proenzyme dormancy by an intrinsic “safety catch” regulatory tripeptide. *Proc Natl Acad Sci US A*. 2001; 98(11):6132–6137.
40. Sadowska A, Car H, Pryczynicz A, Guzinska-Ustymowicz K, Kowal KW, Cepowicz D, Kedra B. Expression of apoptotic proteins in human colorectal cancer and metastatic lymph nodes. *Pathol Res Pract*. 2014; 210(9):576–581. [PubMed: 24939147]
41. Hector S, Conlon S, Schmid J, Dicker P, Cummins RJ, Concannon CG, Johnston PG, Kay EW, Prehn JH. Apoptosome-dependent caspase activation proteins as prognostic markers in Stage II and III colorectal cancer. *Br J Cancer*. 2012; 106(9):1499–1505. [PubMed: 22481083]
42. Peterson QP, Goode DR, West DC, Ramsey KN, Lee JJY, Hergenrother PJ. PAC-1 activates procaspase-3 in vitro through relief of zinc-mediated inhibition. *J Mol Biol*. 2009; 388(1):144–158. [PubMed: 19281821]
43. Peterson QP, Hsu DC, Goode DR, Novotny CJ, Totten RK, Hergenrother PJ. Procaspase-3 activation as an anti-cancer strategy: structure-activity relationship of Procaspase-Activating Compound 1 (PAC-1) and its cellular co-localization with caspase-3. *J Med Chem*. 2009; 52(18):5721–5731. [PubMed: 19708658]
44. Peterson QP, Hsu DC, Novotny CJ, West DC, Kim D, Schmit JM, Dirikolu L, Hergenrother PJ, Fan TM. Discovery and canine preclinical assessment of a nontoxic procaspase-3-activating compound. *Cancer Res*. 2010; 70(18):7232–7241. [PubMed: 20823163]
45. Lucas PW, Schmit JM, Peterson QP, West DC, Hsu DC, Novotny CJ, Dirikolu L, Churchwell MI, Doerge DR, Garrett LD, Hergenrother PJ, Fan TM. Pharmacokinetics and derivation of an anticancer dosing regimen for PAC-1, a preferential small molecule activator of procaspase-3, in healthy dogs. *Invest New Drugs*. 2011; 29(5):901–911. [PubMed: 20499133]
46. Hsu DC, Roth HS, West DC, Botham RC, Novotny CJ, Schmid SC, Hergenrother PJ. Parallel synthesis and biological evaluation of 837 analogues of Procaspase-Activating Compound 1 (PAC-1). *ACS Comb Sci*. 2012; 14(1):44–50. [PubMed: 22007686]
47. West DC, Qin Y, Peterson QP, Thomas DL, Palchadhuri R, Morrison KC, Lucas PW, Palmer AE, Fan TM, Hergenrother PJ. Differential effects of procaspase-3 activating compounds in the induction of cancer cell death. *Mol Pharmaceutics*. 2012; 9(5):1425–1434.
48. Wang F, Wang L, Zhao Y, Li Y, Ping G, Xiao S, Chen K, Zhu W, Gong P, Yang J, Wu C. A novel small-molecule activator of procaspase-3 induces apoptosis in cancer cells and reduces tumor growth in human breast, liver and gallbladder cancer xenografts. *Mol Oncol*. 2014; 8(8):1640–1652. [PubMed: 25053517]
49. Wang F, Liu Y, Wang L, Yang J, Zhao Y, Wang N, Cao Q, Gong P, Wu C. Targeting procaspase-3 with WF-208, a novel PAC-1 derivative, causes selective cancer cell apoptosis. *J Cell Mol Med*. 2015; 19(8):1916–1928. [PubMed: 25754465]
50. Roth HS, Botham RC, Schmid SC, Fan TM, Dirikolu L, Hergenrother PJ. Removal of metabolic liabilities enables development of derivatives of Procaspase-Activating Compound 1 (PAC-1) with improved pharmacokinetics. *J Med Chem*. 2015; 58(9):4046–4065. [PubMed: 25856364]
51. Chakkath T, Lavergne SN, Fan TM, Bunick D, Dirikolu L. Preliminary metabolism of lomustine in dogs and comparative cytotoxicity of lomustine and its major metabolites in canine cells. *Vet Sci*. 2014; 1(3):159–173.
52. Zhang B, Zhao YF, Zhai X, Fan WJ, Ren JL, Wu CF, Gong P. Design, synthesis and antiproliferative activities of diaryl urea derivatives bearing N-acylhydrazone moiety. *Chin Chem Lett*. 2012; 23(8):915–918.

53. Zhang B, Zhao YF, Zhai X, Wang LH, Yang JY, Tan ZH, Gong P. Design, synthesis and anticancer activities of diaryl urea derivatives bearing N-acylhydrazone moiety. *Chem Pharm Bull.* 2012; 60(8):1046–1054. [PubMed: 22863709]
54. Zhai X, Huang Q, Jiang N, Wu D, Zhou HY, Gong P. Discovery of hybrid dual N-acylhydrazone and diaryl urea derivatives as potent antitumor agents: design, synthesis and cytotoxicity evaluation. *Molecules.* 2013; 18(3):2904–2923. [PubMed: 23459301]
55. Huang Q, Fu Q, Liu Y, Bai J, Wang Q, Liao H, Gong P. Design, synthesis and anticancer activity of novel 6-(aminophenyl)-2,4-bismorpholino-1,3,5-triazine derivatives bearing arylmethylene hydrazine moiety. *Chem Res Chin Univ.* 2014; 30(2):257–265.
56. Botham RC, Fan TM, Im I, Borst LB, Dirikolu L, Hergenrother PJ. Dual small-molecule targeting of procaspase-3 dramatically enhances zymogen activation and anticancer activity. *J Am Chem Soc.* 2014; 136(4):1312–1319. [PubMed: 24383395]
57. Ma J, Zhang G, Han X, Bao G, Wang L, Zhai X, Gong P. Synthesis and biological evaluation of benzothiazole derivatives bearing the ortho-hydroxy-N-acylhydrazone moiety as potent antitumor agents. *Arch Pharm Chem Life Sci.* 2014; 347(12):936–949.
58. Ma JJ, Chen D, Lu K, Wang LH, Han XQ, Zhao YF, Gong P. Design, synthesis, and structure-activity relationships of novel benzothiazole derivatives bearing the ortho-hydroxy N-carbamoylhydrazone moiety as potent antitumor agents. *Eur J Med Chem.* 2014; 86:257–269. [PubMed: 25171780]
59. Ma J, Bao G, Wang L, Li W, Xu B, Du B, Lv J, Zhai X, Gong P. Design, synthesis, biological evaluation and preliminary mechanism study of novel benzothiazole derivatives bearing indole-based moiety as potent antitumor agents. *Eur J Med Chem.* 2015; 96:173–186. [PubMed: 25874341]
60. Astrand OAH, Aziz G, Ali SF, Paulsen RE, Hansen TV, Rongved P. Synthesis and initial in vitro biological evaluation of two new zinc-chelating compounds: comparison with TPEN and PAC-1. *Bioorg Med Chem.* 2013; 21(17):5175–5181. [PubMed: 23859779]
61. Bolding Debernard KA, Aziz G, Gjesvik AT, Paulsen RE. Cell death induced by novel procaspase-3 activators can be reduced by growth factors. *Biochem Biophys Res Commun.* 2011; 413(2):364–369. [PubMed: 21893038]
62. Aziz G, Akselsen OW, Hansen TV, Paulsen RE. Procaspase-activating compound 1 induces a caspase-3-dependent cell death in cerebellar granule neurons. *Toxicol Appl Pharmacol.* 2010; 247(3):238–242. [PubMed: 20638399]
63. Qin MZ, Liao WK, Xu C, Fu BL, Ren JG, Gu YC, Gong P. Synthesis and biological evaluation of novel 4-(2-fluorophenoxy)-2-(1H-tetrazol-1-yl)pyridines bearing semicarbazone moieties as potent antitumor agents. *Arch Pharm Chem Life Sci.* 2013; 346(11):840–850.
64. Luo H, Yang C, Zhang X, Zhao M, Jiang D, Xiao J, Yang X, Li S. Design, synthesis, and antitumor activity of a novel series of PAC-1 analogues. *Chem Res Chin Univ.* 2013; 29(5):906–910.
65. Razi SS, Schwartz G, Boone D, Li X, Belsley S, Todd G, Connery CP, Bhora FY. Small molecule activation of procaspase-3 induces apoptosis in human lung adenocarcinoma: a tailored anti-cancer strategy. *J Surg Res.* 2010; 158(2):402–403.
66. Razi SS, Rehmani S, Li X, Park K, Schwartz GS, Latif MJ, Bhora FY. Antitumor activity of paclitaxel is significantly enhanced by a novel proapoptotic agent in non small cell lung cancer. *J Surg Res.* 2015; 194(2):622–630. [PubMed: 25498514]
67. Zhao HJ, Liu T, Mao X, Han SX, Liang RX, Hui LQ, Cao CY, You Y, Zhang LZ. Fructus phyllanthi tannin fraction induces apoptosis and inhibits migration and invasion of human lung squamous carcinoma cells in vitro via MAPK/MMP pathways. *Acta Pharmacol Sin.* 2015; 36(6):758–768. [PubMed: 25864648]
68. Xu J, Li Z, Wang J, Chen H, Fang JY. Combined PTEN mutation and protein expression associate with overall and disease-free survival of glioblastoma patients. *Transl Oncol.* 2014; 7(2):196–205. [PubMed: 24721394]
69. Razi SS, Schwartz G, Li XG, Boone D, Belsley S, Todd G, Connery CP, Bhora FY. Direct activation of procaspase-3 inhibits human lung adenocarcinoma in a murine model. *J Am Coll Surgeons.* 2010; 211(3):S36–S36.

70. Zorn JA, Wille H, Wolan DW, Wells JA. Self-assembling small molecules form nanofibrils that bind procaspase-3 to promote activation. *J Am Chem Soc.* 2011; 133(49):19630–3. [PubMed: 22066605]
71. Zorn JA, Wolan DW, Agard NJ, Wells JA. Fibrils colocalize caspase-3 with procaspase-3 to foster maturation. *J Biol Chem.* 2012; 287(40):33781–33795. [PubMed: 22872644]
72. Julien O, Kampmann M, Bassik MC, Zorn JA, Venditto VJ, Shimbo K, Agard NJ, Shimada K, Rheingold AL, Stockwell BR, Weissman JS, Wells JA. Unraveling the mechanism of cell death induced by chemical fibrils. *Nat Chem Biol.* 2014; 10(11):969–976. [PubMed: 25262416]
73. Charkoudian LK, Pham DM, Franz KJ. A pro-chelator triggered by hydrogen peroxide inhibits iron-promoted hydroxyl radical formation. *J Am Chem Soc.* 2006; 128(38):12424–12425. [PubMed: 16984186]
74. Johnson DK, Murphy TB, Rose NJ, Goodwin WH, Pickart L. Cytotoxic chelators and chelates. 1. Inhibition of DNA synthesis in cultured rodent and human cells by aroylhydrazones and by a copper(II) complex of salicylaldehyde benzoyl hydrazone. *Inorg Chim Acta.* 1982; 67(5):159–165.
75. Peng X, Tang X, Qin W, Dou W, Guo Y, Zheng J, Liu W, Wang D. Aroylhydrazone derivative as fluorescent sensor for highly selective recognition of Zn²⁺ ions: syntheses, characterization, crystal structures and spectroscopic properties. *Dalton Trans.* 2011; 40(19):5271–5277. [PubMed: 21468436]
76. Muzio M, Salvesen GS, Dixit VM. FLICE induced apoptosis in a cell-free system. Cleavage of caspase zymogens. *J Biol Chem.* 1997; 272(5):2952–2956. [PubMed: 9006941]
77. Perry DK, Smyth MJ, Stennicke HR, Salvesen GS, Duriez P, Poirier GG, Hannun YA. Zinc is a potent inhibitor of the apoptotic protease, caspase-3. A novel target for zinc in the inhibition of apoptosis. *J Biol Chem.* 1997; 272(30):18530–18533. [PubMed: 9228015]
78. Huber KL, Hardy JA. Mechanism of zinc-mediated inhibition of caspase-9. *Protein Sci.* 2012; 21(7):1056–1065. [PubMed: 22573662]
79. Velazquez-Delgado EM, Hardy JA. Zinc-mediated allosteric inhibition of caspase-6. *J Biol Chem.* 2012; 287(43):36000–36011. [PubMed: 22891250]
80. Truong-Tran AQ, Grosser D, Ruffin RE, Murgia C, Zalewski PD. Apoptosis in the normal and inflamed airway epithelium: role of zinc in epithelial protection and procaspase-3 regulation. *Biochem Pharmacol.* 2003; 66(8):1459–1468. [PubMed: 14555222]
81. Daniel AG, Peterson EJ, Farrell NP. The bioinorganic chemistry of apoptosis: potential inhibitory zinc binding sites in caspase-3. *Angew Chem Int Ed Engl.* 2014; 53(16):4098–4101. [PubMed: 24643997]
82. Guo WT, Wang XW, Yan YL, Li YP, Yin X, Zhang Q, Melton C, Shenoy A, Reyes NA, Oakes SA, Blesch R, Wang Y. Suppression of epithelial-mesenchymal transition and apoptotic pathways by miR-294/302 family synergistically blocks let-7-induced silencing of self-renewal in embryonic stem cells. *Cell Death Differ.* 2015; 22(7):1158–1169. [PubMed: 25501598]
83. Campbell DS, Okamoto H. Local caspase activation interacts with Slit-Robo signaling to restrict axonal arborization. *J Cell Biol.* 2013; 203(4):657–672. [PubMed: 24385488]
84. Monaco G, Decrock E, Akl H, Ponsaerts R, Vervliet T, Luyten T, De Maeyer M, Missiaen L, Distelhorst CW, De Smedt H, Parys JB, Leybaert L, Bultynck G. Selective regulation of IP3-receptor-mediated Ca²⁺ signaling and apoptosis by the BH4 domain of Bcl-2 versus Bcl-X_L. *Cell Death Differ.* 2012; 19(2):295–309. [PubMed: 21818117]
85. Putinski C, Abdul-Ghani M, Stiles R, Brunette S, Dick SA, Fernando P, Megeney LA. Intrinsic-mediated caspase activation is essential for cardiomyocyte hypertrophy. *Proc Natl Acad Sci US A.* 2013; 110(43):E4079–E4087.
86. Dong T, Zhang Q, Hamblin MR, Wu MX. Low-level light in combination with metabolic modulators for effective therapy of injured brain. *J Cereb Blood Flow Metab.* 2015; 35(9):1435–1444. [PubMed: 25966949]
87. Dick SA, Chang NC, Dumont NA, Bell RA, Putinski C, Kawabe Y, Litchfield DW, Rudnicki MA, Megeney LA. Caspase 3 cleavage of Pax7 inhibits self-renewal of satellite cells. *Proc Natl Acad Sci US A.* 2015; 112(38):E5246–E5252.

88. Seervi M, Sobhan PK, Mathew KA, Joseph J, Pillai PR, Santhoshkumar TR. A high-throughput image-based screen for the identification of Bax/Bak-independent caspase activators against drug-resistant cancer cells. *Apoptosis*. 2014; 19(1):269–284. [PubMed: 24220853]
89. Sjolli S, Solli AI, Akselsen O, Jiang Y, Berg E, Hansen TV, Sylte I, Winberg JO. PAC-1 and isatin derivatives are weak matrix metalloproteinase inhibitors. *Biochim Biophys Acta*. 2014; 1840(10): 3162–3169. [PubMed: 25046380]
90. Baell JB, Holloway GA. New substructure filters for removal of pan assay interference compounds (PAINS) from screening libraries and for their exclusion in bioassays. *J Med Chem*. 2010; 53(7): 2719–2740. [PubMed: 20131845]
91. Makhov P, Golovine K, Uzzo RG, Rothman J, Crispin PL, Shaw T, Scoll BJ, Kolenko VM. Zinc chelation induces rapid depletion of the X-linked inhibitor of apoptosis and sensitizes prostate cancer cells to TRAIL-mediated apoptosis. *Cell Death Differ*. 2008; 15(11):1745–1751. [PubMed: 18617897]
92. Hepowit NL, Uthandi S, Miranda HV, Toniutti M, Prunetti L, Olivarez O, De Vera IM, Fanucci GE, Chen S, Maupin-Furlow JA. Archaeal JAB1/MPN/MOV34 metalloenzyme (HvJAMM1) cleaves ubiquitin-like small archaeal modifier proteins (SAMPs) from protein-conjugates. *Mol Microbiol*. 2012; 86(4):971–987. [PubMed: 22970855]
93. Lee HG, Lee JH, Jang SP, Park HM, Kim SJ, Kim Y, Kim C, Harrison RG. Zinc selective chemosensor based on pyridyl-amide fluorescence. *Tetrahedron*. 2011; 67(42):8073–8078.
94. Richardson DR, Hefter GT, May PM, Webb J, Baker E. Iron chelators of the pyridoxal isonicotinoyl hydrazone class. III. Formation constants with calcium(II), magnesium(II) and zinc(II). *Biol Metals*. 1989; 2(3):161–167.
95. Jänicke RU, Sprengart ML, Wati MR, Porter AG. Caspase-3 is required for DNA fragmentation and morphological changes associated with apoptosis. *J Biol Chem*. 1998; 273(16):9357–9360. [PubMed: 9545256]
96. Peterson QP, Goode DR, West DC, Botham RC, Hergenrother PJ. Preparation of the caspase-3/7 substrate Ac-DEVD-pNA by solution-phase peptide synthesis. *Nat Protoc*. 2010; 5(2):294–302. [PubMed: 20134429]
97. Westphal MV, Wolfstader BT, Plancher JM, Gatfield J, Carreira EM. Evaluation of *tert*-butyl isosteres: Case studies of physicochemical and pharmacokinetic properties, efficacies, and activities. *ChemMedChem*. 2015; 10(3):461–469. [PubMed: 25630804]
98. Ren L, Bi K, Gong P, Cheng W, Song Z, Fang L, Chen X. Characterization of the in vivo and in vitro metabolic profile of PAC-1 using liquid chromatography mass spectrometry. *J Chromatogr B*. 2008; 876(1):47–53.
99. Soars MG, Gelboin HV, Krausz KW, Riley RJ. A comparison of relative abundance, activity factor and inhibitory monoclonal antibody approaches in the characterization of human CYP enzymology. *Br J Clin Pharmacol*. 2003; 55(2):175–181. [PubMed: 12580989]
100. Huang S, Clark RJ, Zhu L. Highly sensitive fluorescent probes for zinc ion based on triazolyl-containing tetradentate coordination motifs. *Org Lett*. 2007; 9(24):4999–5002. [PubMed: 17956110]
101. Cecchelli R, Berezowski V, Lundquist S, Culot M, Renftel M, Dehouck MP, Fenart L. Modelling of the blood-brain barrier in drug discovery and development. *Nat Rev Drug Discov*. 2007; 6(8): 650–661. [PubMed: 17667956]
102. Qin Y, Dittmer PJ, Park JG, Jansen KB, Palmer AE. Measuring steady-state and dynamic endoplasmic reticulum and Golgi Zn²⁺ with genetically encoded sensors. *Proc Natl Acad Sci US A*. 2011; 108(18):7351–7356.
103. Rae JM, Creighton CJ, Meck JM, Haddad BR, Johnson MD. MDA-MB-435 cells are derived from M14 melanoma cells--a loss for breast cancer, but a boon for melanoma research. *Breast Cancer Res Treat*. 2007; 104(1):13–19. [PubMed: 17004106]
104. Cossu F, Malvezzi F, Canevari G, Mastrangelo E, Lecis D, Delia D, Seneci P, Scolastico C, Bolognesi M, Milani M. Recognition of Smac-mimetic compounds by the BIR domain of cIAP1. *Protein Sci*. 2010; 19(12):2418–2429. [PubMed: 20954235]
105. Joshi, AD.; Botham, RC.; Roth, HS.; Fan, TM.; Tarasow, TM.; Hergenrother, PJ.; Riggins, GJ. An oral procaspase activating drug, PAC-1, shows preclinical promise for glioblastoma therapy.

Proceedings of the 106th Annual Meeting of the American Association for Cancer Research; Philadelphia, PA. April 18–22, 2015; Philadelphia, PA: 2015. p. 3620

Author Manuscript

Author Manuscript

Author Manuscript

Author Manuscript

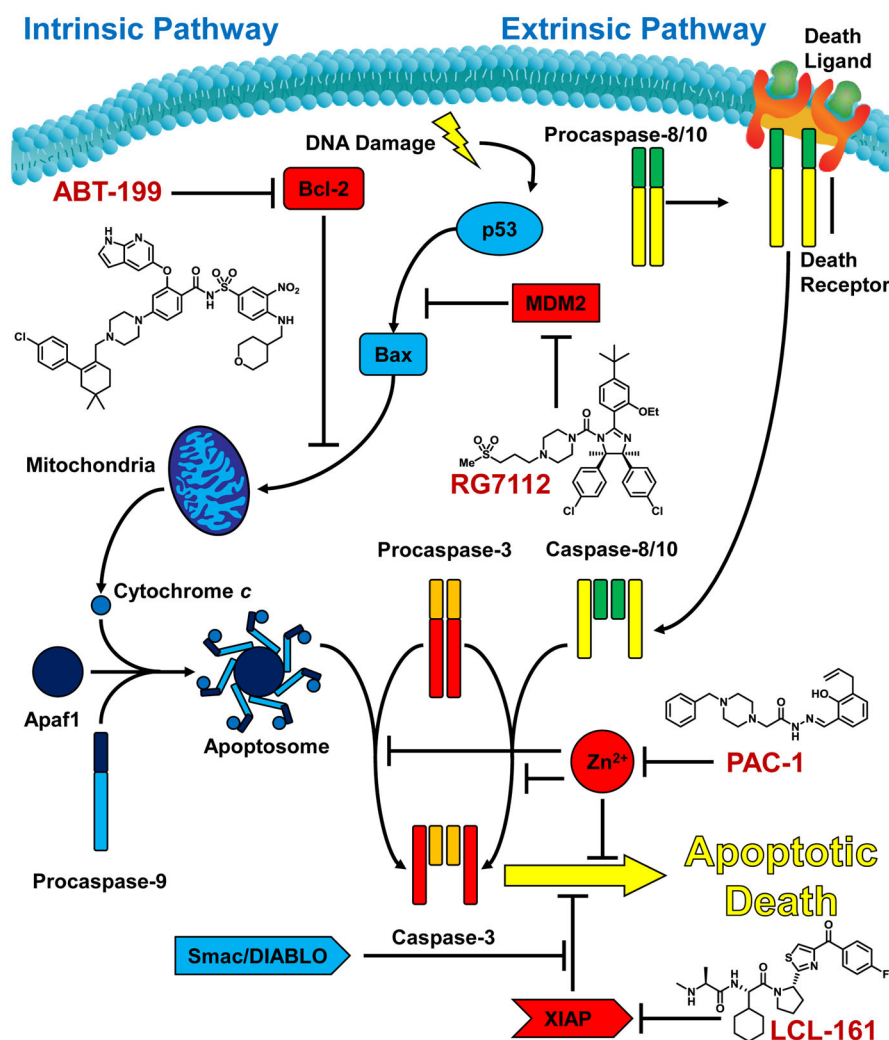


Figure 1. Inhibiting endogenous antiapoptotic processes as a means of drug-mediated activation of apoptosis. Cellular inhibitors of apoptosis are shown in red: MDM2 binds to p53, preventing its proapoptotic effect; Bcl-2 binds Bax, inhibiting the proapoptotic action of Bax on the mitochondria; XIAP binds to and inhibits caspase-3, preventing the caspase-3 mediated cleavage of cellular substrates; and Zn²⁺ binds to and inhibits the enzymatic activity of procaspase-3 and caspase-3, inhibiting both procaspase-3 activation and caspase-3 mediated cleavage of cellular substrates. Representative small-molecule modulators of MDM2, Bcl-2, XIAP, and Zn²⁺ (RG7112, ABT-199, LCL-161 and PAC-1, respectively) are shown.

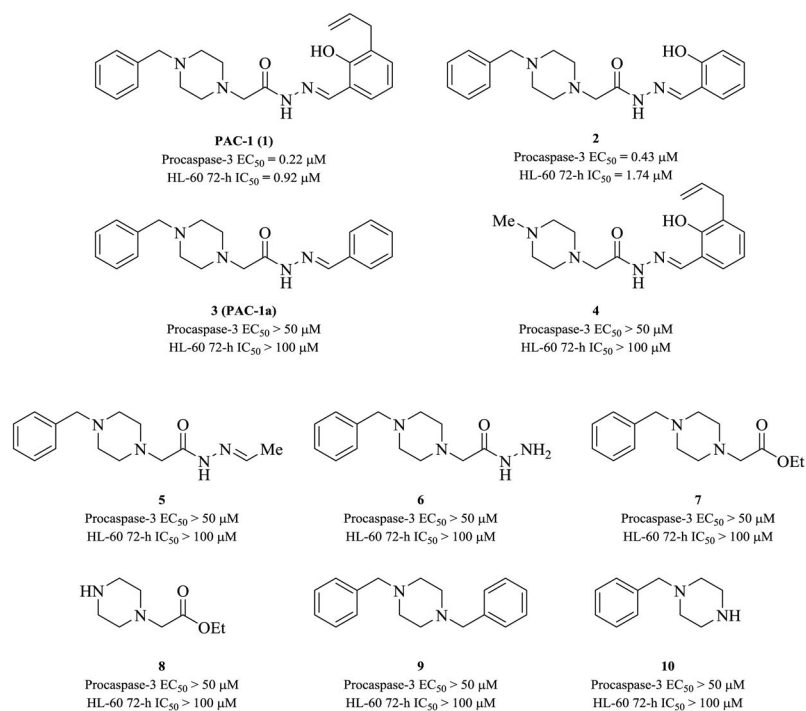


Figure 2.
 Preliminary SAR studies of **PAC-1**. [15]

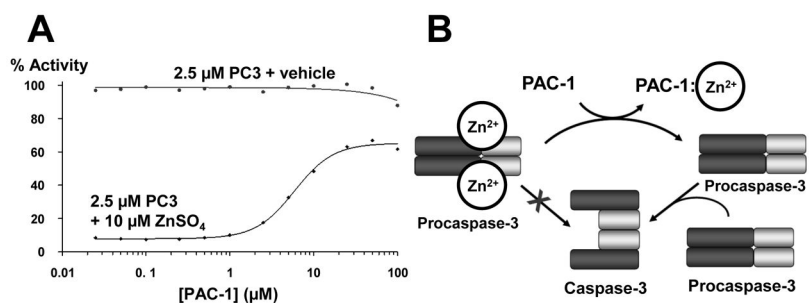


Figure 3.

A. PAC-1 has no effect on procaspase-3 in a metal-free buffer but relieves zinc-mediated inhibition of procaspase-3 in a dose-dependent manner. **B.** Proposed mechanism of action of PAC-1. PAC-1 chelates labile zinc from procaspase-3, facilitating activation to caspase-3. Figures adapted from: Peterson, Q.P., *et al.*, PAC-1 activates procaspase-3 *in vitro* through relief of zinc-mediated inhibition, *J. Mol. Biol.*, **2009**, *388*(1), 144–158, Copyright © 2009, with permission from Elsevier. [42]

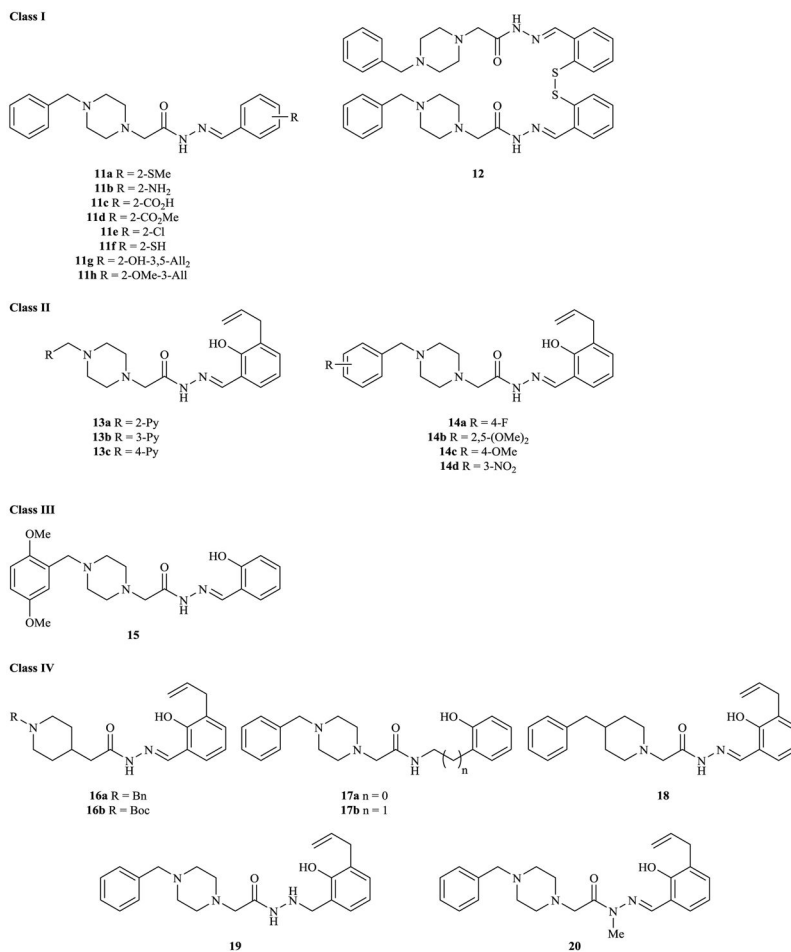


Figure 4. Four classes of **PAC-1** derivatives synthesized for SAR determination. Pyr = pyridyl [43]

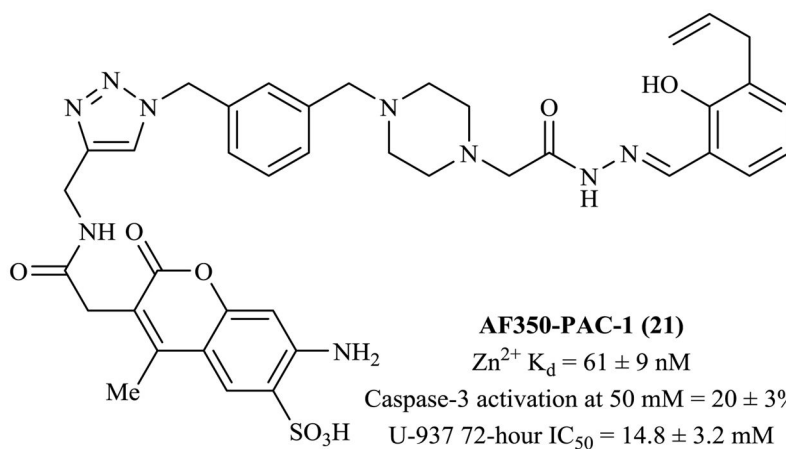


Figure 5.
Structure of fluorescent **PAC-1** derivative **21**. [43]

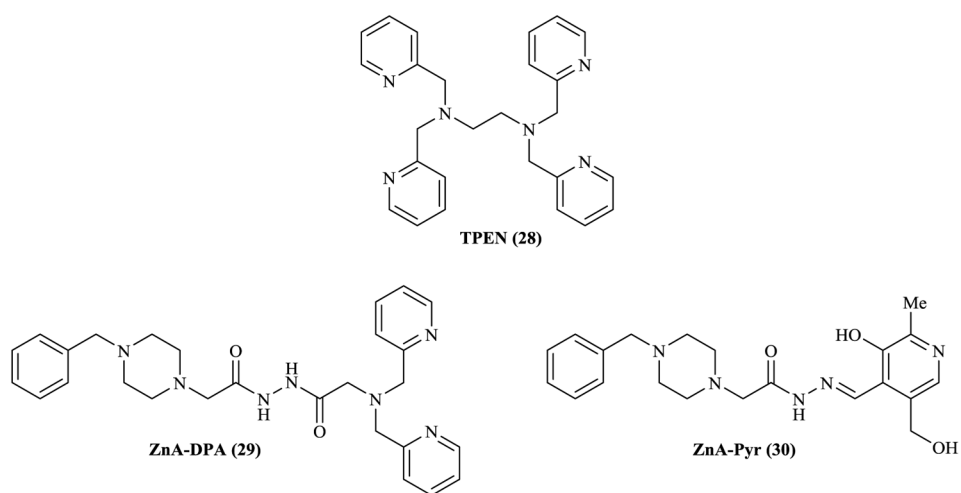


Figure 6. Structures of **TPEN (28)** and **PAC-1** derivatives **ZnA-DPA (29)** and **ZnA-Pyr (30)**. [60]

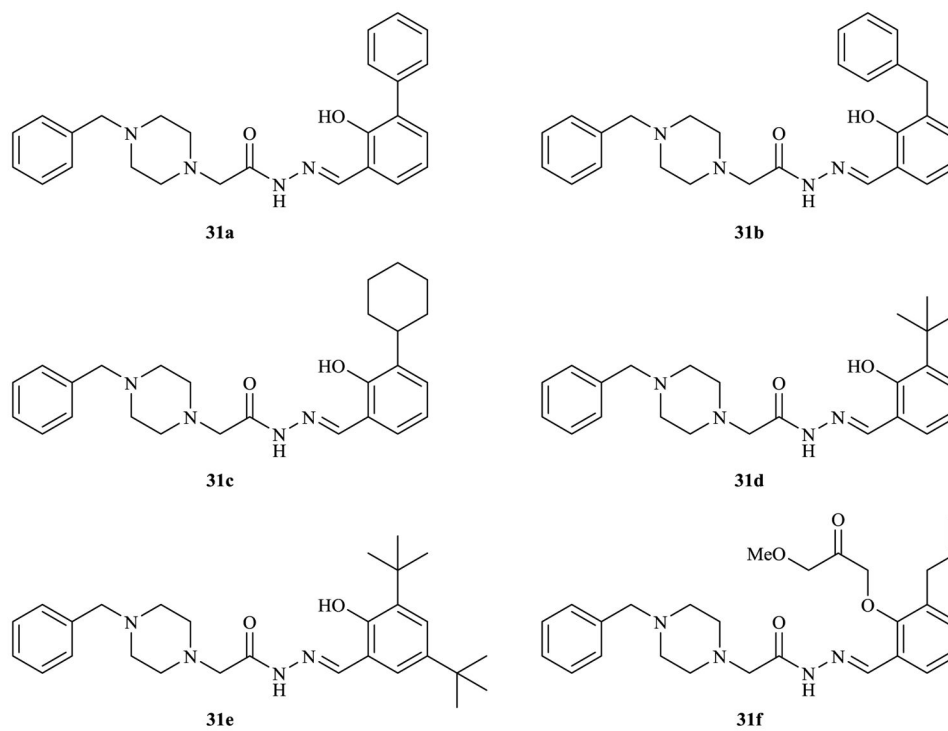
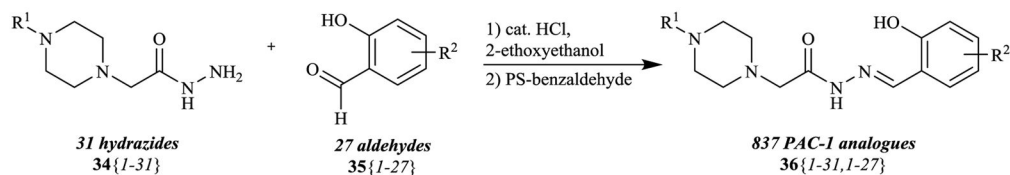
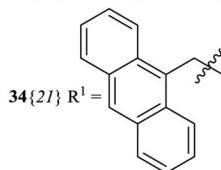


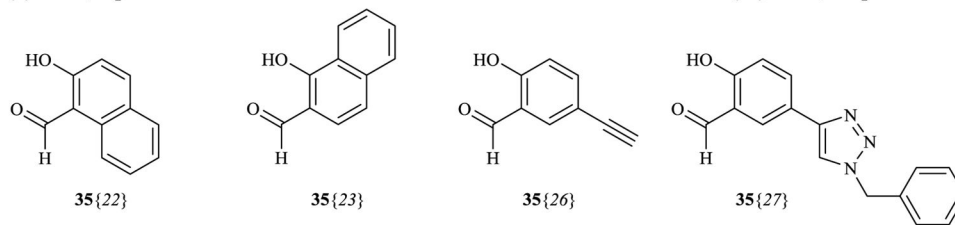
Figure 7. Structures of compounds (**31a-f**) used to study matrix metalloproteinase inhibition. [89]

**Hydrazides:**

- | | | |
|--|---|---|
| 34{1} R ¹ = Bn | 34{11} R ¹ = CH ₂ (3-OPh-Ph) | 34{22} R ¹ = CH ₂ (3,5-(<i>t</i> -Bu) ₂ -Ph) |
| 34{2} R ¹ = CH ₂ (4-OMe-Ph) | 34{12} R ¹ = CH ₂ (2-Ph-Ph) | 34{23} R ¹ = CHPh ₂ |
| 34{3} R ¹ = CH ₂ (3-NO ₂ -Ph) | 34{13} R ¹ = CH ₂ (4-Me-Ph) | 34{24} R ¹ = CH ₂ (1-Nap) |
| 34{4} R ¹ = CH ₂ (2,5-(OMe) ₂ -Ph) | 34{14} R ¹ = CH ₂ (2,3,4,5,6-Me ₅ -Ph) | 34{25} R ¹ = CH ₂ (2-Nap) |
| 34{5} R ¹ = CH ₂ (4-SO ₂ NH ₂ -Ph) | 34{15} R ¹ = CH ₂ (4-CF ₃ -Ph) | 34{26} R ¹ = CH ₂ (Ph)(4-Cl-Ph) |
| 34{6} R ¹ = CH ₂ (3-CH ₂ N ₃ -Ph) | 34{16} R ¹ = CH ₂ (3,4,5-(OMe) ₃ -Ph) | 34{27} R ¹ = CH ₂ (2- <i>i</i> -Ph) |
| 34{7} R ¹ = CH ₂ (2-Cl-6-F-Ph) | 34{17} R ¹ = CH ₂ (4-OCF ₃ -Ph) | 34{28} R ¹ = CH ₂ (4-Et-Ph) |
| 34{8} R ¹ = CH ₂ (3-Cl-Ph) | 34{18} R ¹ = CH ₂ (4-OBn-Ph) | 34{29} R ¹ = CH ₂ (2-(CH ₂ SO ₂ Ph)-Ph) |
| 34{9} R ¹ = CH ₂ (4-Br-Ph) | 34{19} R ¹ = CH ₂ (4- <i>i</i> -Pr-Ph) | 34{30} R ¹ = Ph |
| 34{10} R ¹ = CH ₂ (3,4-(OBn) ₂ -Ph) | 34{20} R ¹ = CH ₂ (4- <i>t</i> -Bu-Ph) | 34{31} R ¹ = CH ₂ (4-Bz-Ph) |

**Aldehydes:**

- | | | |
|---|--|---|
| 35{1} = salicylaldehyde | 35{9} R ² = 3,5-I ₂ | 35{16} R ² = 4,6-(OMe) ₂ |
| 35{2} R ² = 3-OMe | 35{10} R ² = 4-OBn | 35{17} R ² = 3-OMe-6-Br |
| 35{3} R ² = 5-Br | 35{11} R ² = 3-OEt | 35{18} R ² = 3,5-Cl ₂ |
| 35{4} R ² = 4-NEt ₂ | 35{12} R ² = 3-OH | 35{19} R ² = 4-OH-6-Me |
| 35{5} R ² = 5-OCF ₃ | 35{13} R ² = 3-Me-5-Cl | 35{20} R ² = 3,5-(NO ₂) ₂ |
| 35{6} R ² = 3-Cl | 35{14} R ² = 3,5-Br ₂ -4-OMe | 35{21} R ² = 3,5-Br ₂ |
| 35{7} R ² = 3,5-(<i>t</i> -Bu) ₂ | 35{15} R ² = 5-NO ₂ | 35{24} R ² = 3-All |
| 35{8} R ² = 3,5-F ₂ | | 35{25} R ² = 3,5-All ₂ |

**Figure 8.**

Hydrazides and aldehydes used to construct 837-membered combinatorial library of **PAC-1** analogues. Figure adapted with permission from: Hsu, D.C., *et al.* Parallel synthesis and biological evaluation of 837 analogues of Procaspase-Activating Compound 1 (**PAC-1**). *ACS Comb. Sci.* **2012**, *14* (1), 44–50. Copyright © 2012 American Chemical Society. [46]

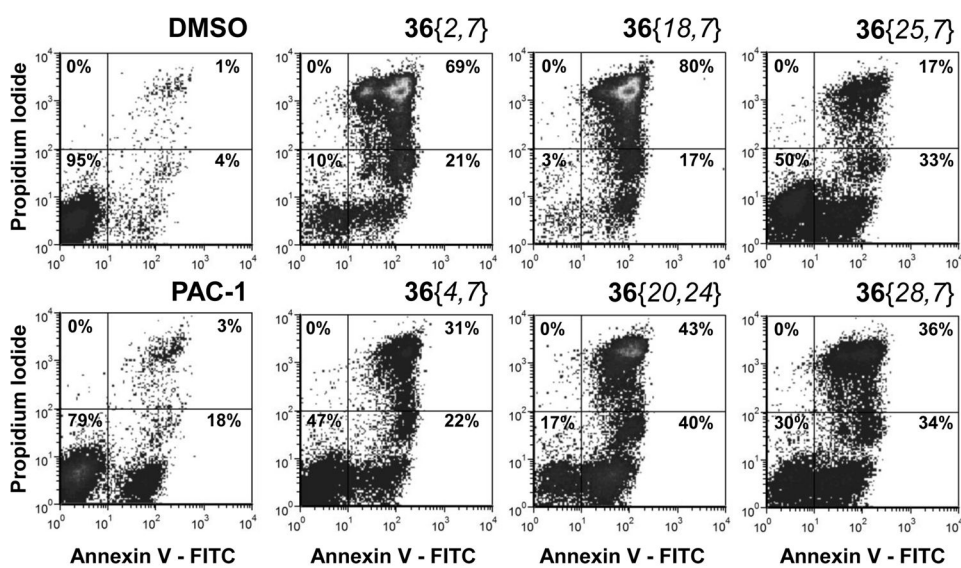


Figure 9. Annexin V-FITC/propidium iodide staining of U-937 cells treated with 7.5 μ M of each compound for 24 hours. [46]

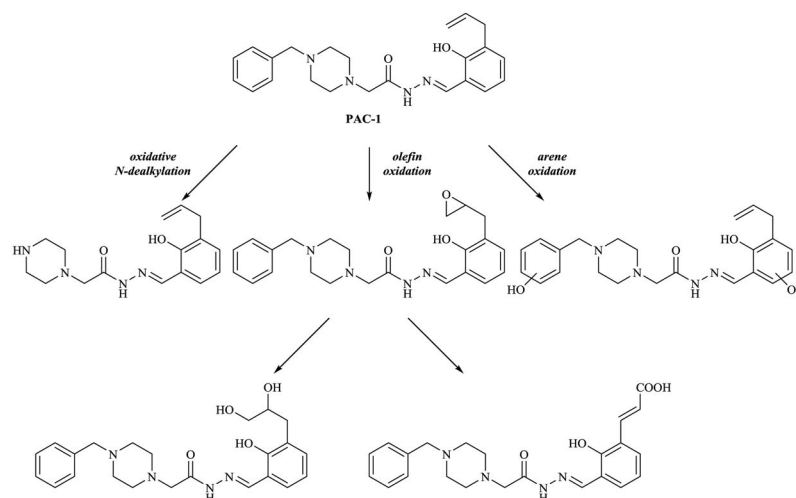
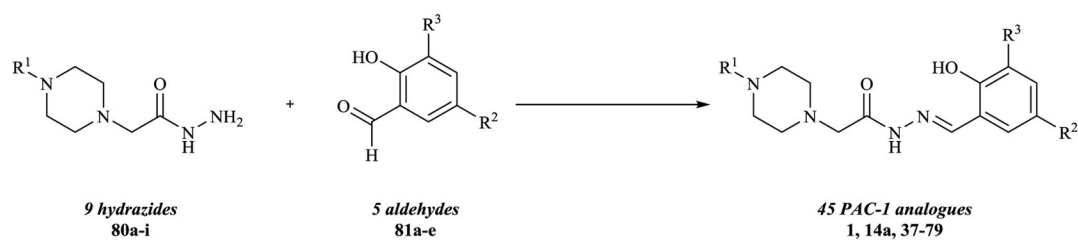
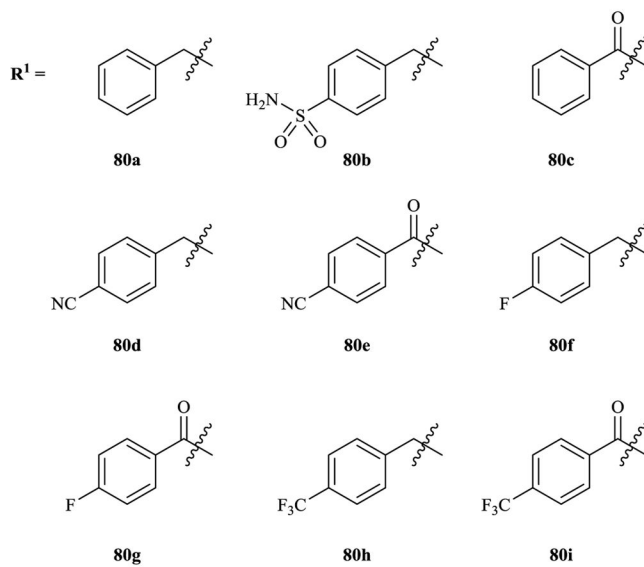
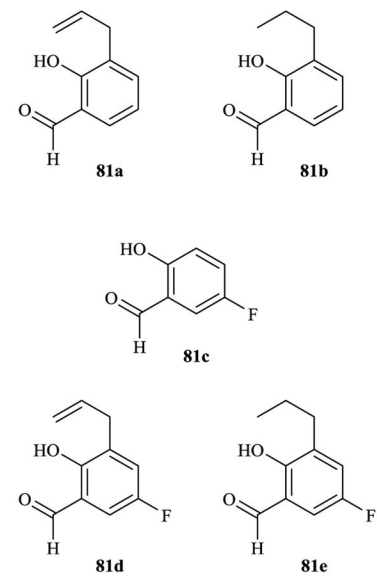


Figure 10.

PAC-1 is susceptible to enzymatic oxidation *in vitro* and *in vivo*, giving metabolites that result from *N*-dealkylation, olefin oxidation, and arene oxidation. Figure adapted with permission from: Roth, H.S., *et al.* Removal of metabolic liabilities enables development of derivatives of Procaspase-Activating Compound 1 (PAC-1) with improved pharmacokinetics. *J. Med. Chem.* **2015**, *58*(9), 4046–4065. Copyright © 2015 American Chemical Society. [50, 98]

**Hydrazides****Aldehydes****Figure 11.**

Nine hydrazides and five aldehydes were used to construct a library of 45 **PAC-1** derivatives designed to display enhanced metabolic stability by blocking oxidative *N*-dealkylation, olefin oxidation, and/or arene oxidation. Figure adapted with permission from: Roth, H.S., *et al.* Removal of metabolic liabilities enables development of derivatives of Procaspase-Activating Compound 1 (**PAC-1**) with improved pharmacokinetics. *J. Med. Chem.* **2015**, *58*(9), 4046–4065. Copyright © 2015 American Chemical Society. [50]

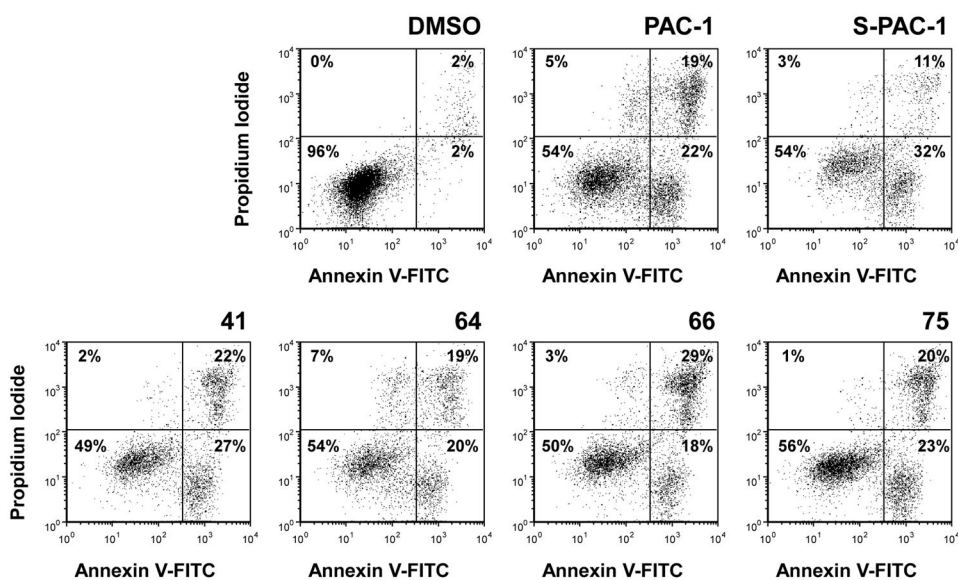


Figure 12.

PAC-1 and derivatives induce apoptosis in U-937 cells. Cells were treated for 12 hours at 50 μ M, and viability was assessed by Annexin V-FITC/propidium iodide staining. Data shown are representative of three independent experiments. Figure adapted with permission from: Roth, H.S., *et al.* Removal of metabolic liabilities enables development of derivatives of Procaspase-Activating Compound 1 (**PAC-1**) with improved pharmacokinetics. *J. Med. Chem.* **2015**, *58*(9), 4046–4065. Copyright © 2015 American Chemical Society. [50]

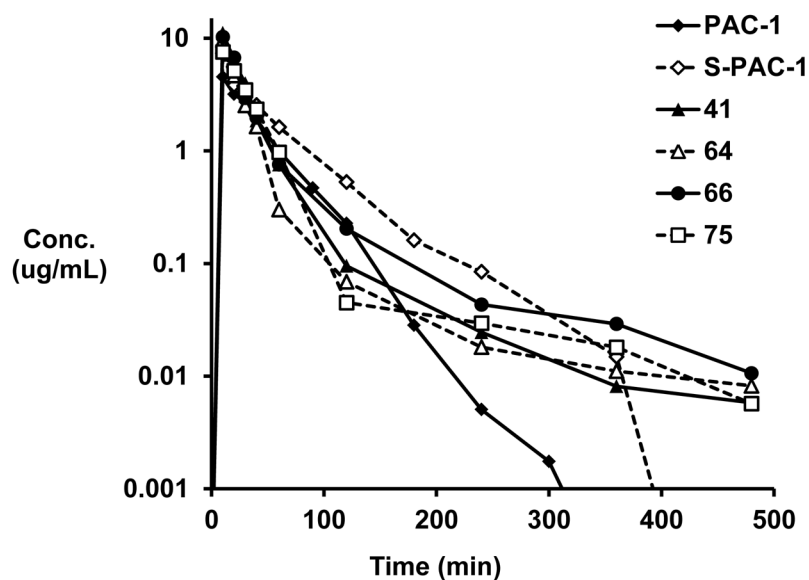


Figure 13.

Pharmacokinetic profiles of **PAC-1** and selected derivatives following 25 mg/kg intravenous dose ($n = 2$). Detectable levels of the novel derivatives are present in serum for at least 8 hours post-treatment, while **PAC-1** and **S-PAC-1** are no longer detectable after 5 and 6 hours post-treatment, respectively. Figure adapted with permission from: Roth, H.S., *et al.* Removal of metabolic liabilities enables development of derivatives of Procaspase-Activating Compound 1 (**PAC-1**) with improved pharmacokinetics. *J. Med. Chem.* **2015**, *58*(9), 4046–4065. Copyright © 2015 American Chemical Society. [50]

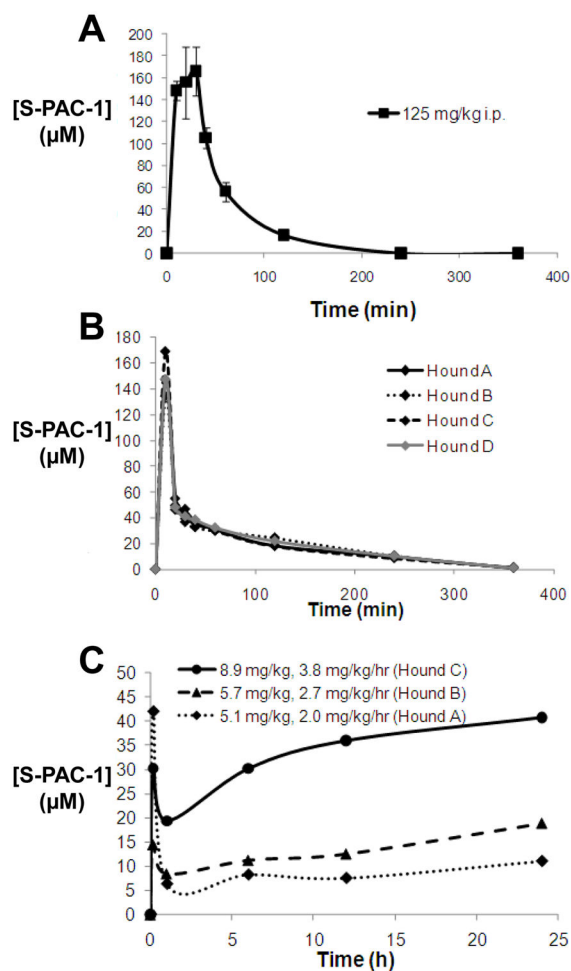


Figure 14. Pharmacokinetics of S-PAC-1 following **A.** 125 mg/kg i.p. injection in mice, **B.** 25 mg/kg i.v. injection in dogs administered over 10 minutes, and **C.** initial loading dose followed by 24-hour continuous rate infusion in dogs administered by i.v. injection. Figures adapted with permission from: Peterson, Q.P., *et al.* Discovery and canine preclinical assessment of a nontoxic procaspase-3 activating compound. *Cancer Res.* **2010**, *70*(18), 7232–7241. Copyright © 2010 American Association for Cancer Research. [44]

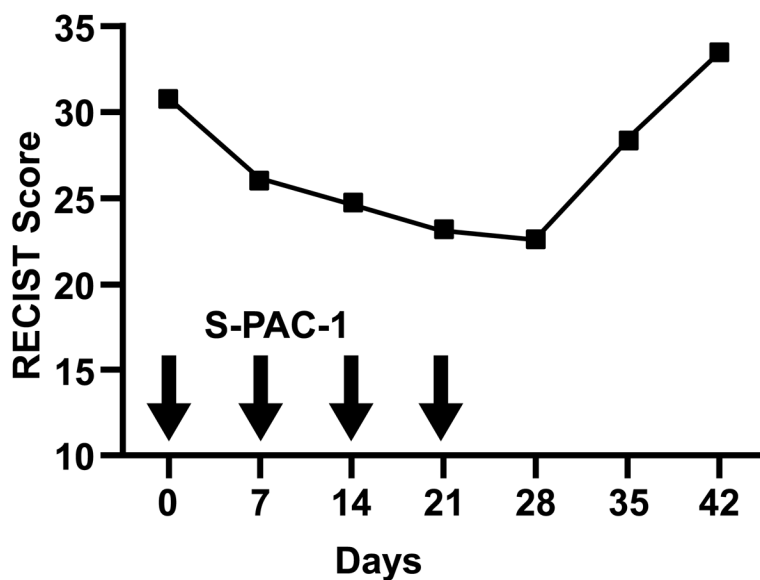


Figure 15.

Partial response to **S-PAC-1** therapy in a canine lymphoma patient. RECIST scores for patient administered **S-PAC-1** on days 0, 7, 14, and 21. Tumor size decreased upon each dose and rapidly increased upon cessation of treatment. Figure adapted with permission from: Peterson, Q.P., *et al.* Discovery and canine preclinical assessment of a nontoxic procaspase-3 activating compound. *Cancer Res.* **2010**, *70*(18), 7232–7241. Copyright © 2010 American Association for Cancer Research. [44]

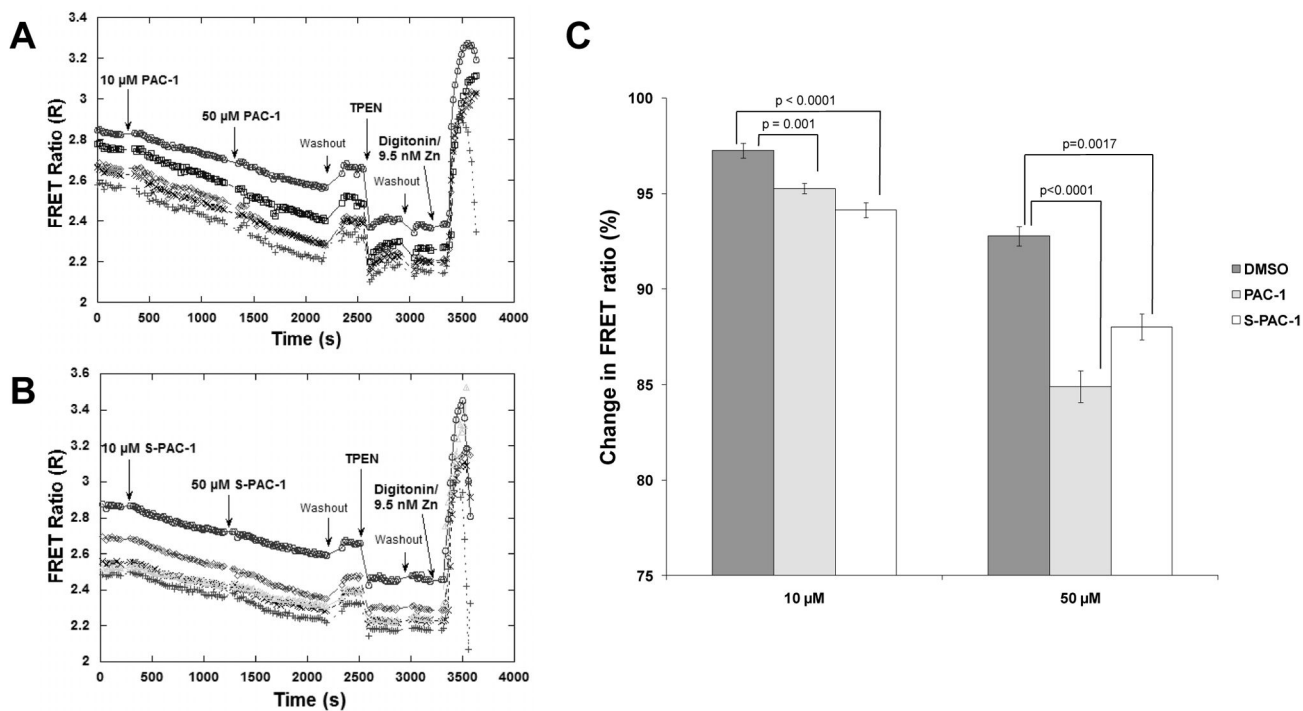


Figure 16.

Changes in intracellular zinc concentration upon treatment with **A. PAC-1** or **B. S-PAC-1**.

C. Both **PAC-1** and **S-PAC-1** cause significant decreases in intracellular zinc concentration compared to untreated controls. Figures adapted with permission from literature. Figures adapted with permission from: West, D.C., *et al.* Differential effects of procaspase-3 activating compounds in the induction of cancer cell death. *Mol. Pharmaceutics* **2012**, *9*(5), 1425–1434. Copyright © 2012 American Chemical Society. [47]

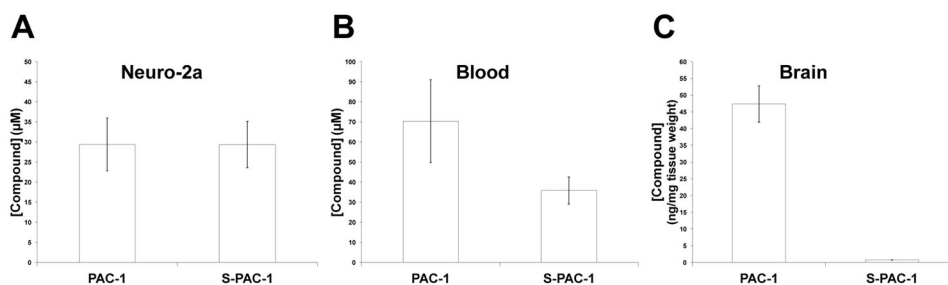


Figure 17.

Penetration of physiological barriers by **PAC-1** and **S-PAC-1**. **A.** Concentrations of **PAC-1** and **S-PAC-1** in Neuro-2a cells following treatment with 50 μM for 30 minutes. **B.** Concentrations of **PAC-1** and **S-PAC-1** in serum, and **C.** concentrations of **PAC-1** and **S-PAC-1** in brains of mice. C57BL/6 mice received **PAC-1** or **S-PAC-1** at 75 mg/kg via lateral tail vein injection and sacrificed 5 minutes post-injection. Values shown are mean \pm standard deviation ($n = 4$). Figures adapted with permission from: West, D.C., *et al.* Differential effects of procaspase-3 activating compounds in the induction of cancer cell death. *Mol. Pharmaceutics* **2012**, *9*(5), 1425–1434. Copyright © 2012 American Chemical Society. [47]

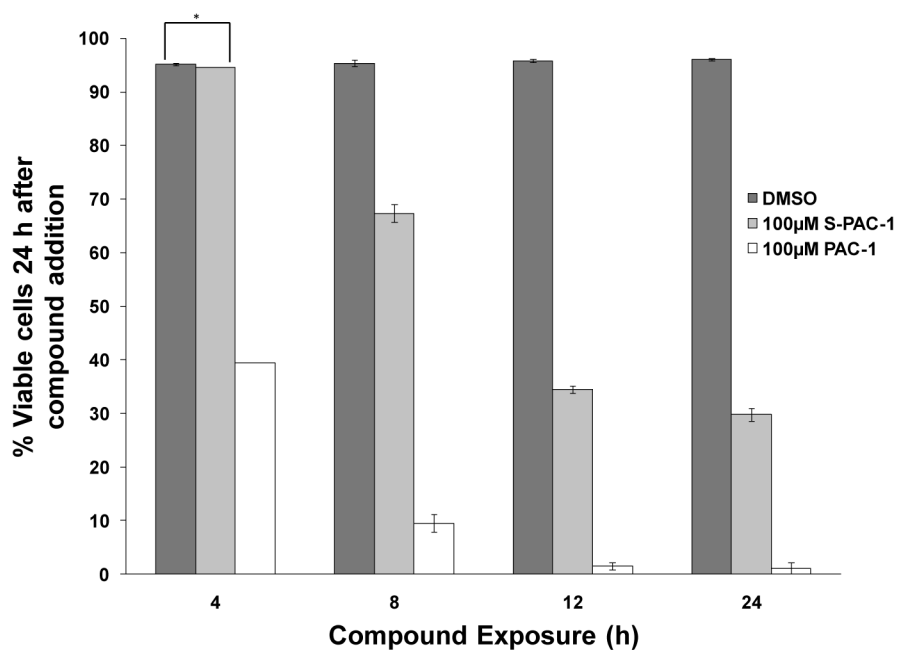


Figure 18.

High concentrations of **PAC-1**, but not **S-PAC-1**, induce apoptosis upon short treatment times. U-937 cells were treated with DMSO or compound (100 μM) for various exposure times, and cell viability was assessed by flow cytometry of the cells double stained with Annexin V-FITC/propidium iodide. Values shown are mean ± s.e.m. (n = 3). Figure adapted with permission from: West, D.C., *et al.* Differential effects of procaspase-3 activating compounds in the induction of cancer cell death. *Mol. Pharmaceutics* **2012**, *9*(5), 1425–1434. Copyright © 2012 American Chemical Society. [47]

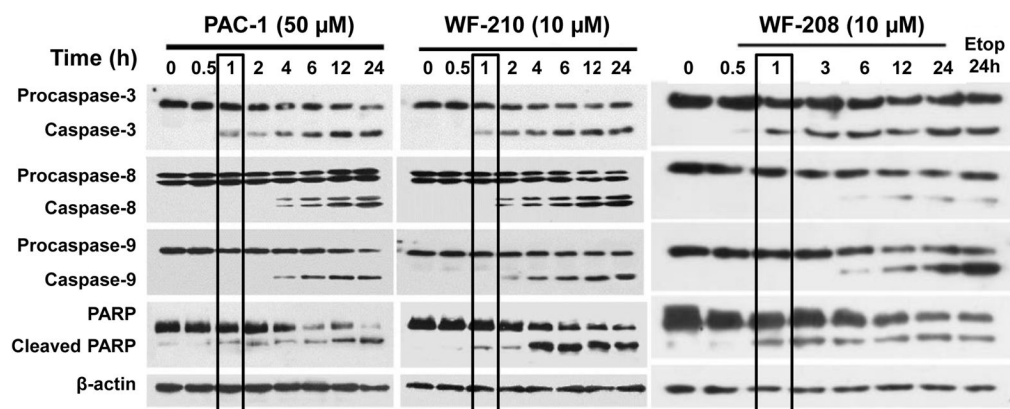


Figure 19.

Activation of caspases in HL-60 cells by **PAC-1**, **WF-210**, and **WF-208**. Cells were treated with compounds for 24 hours. Cleavage of caspase-3 and PARP were detected first, followed by caspases-8 and -9 (boxes). Etop = etoposide. Figures adapted with permission from: Wang, F., *et al.* A novel small-molecule activator of procaspase-3 induces apoptosis in cancer cells and reduces tumor growth in human breast, liver and gallbladder cancer xenografts. *Mol. Oncol.* **2014**, *8*(8), 1640–1652. Copyright © 2014 Federation of European Biochemical Societies; Wang, F., *et al.* Targeting procaspase-3 with WF-208, a novel PAC-1 derivative, causes selective cancer cell apoptosis. *J. Cell. Mol. Med.* **2015**, *19*(8), 1916–1928. Copyright © 2015 The Authors. [48, 49]

Table 1Zinc chelation, *in vitro* caspase-3 activation, and cytotoxicity of **PAC-1** and derivatives.

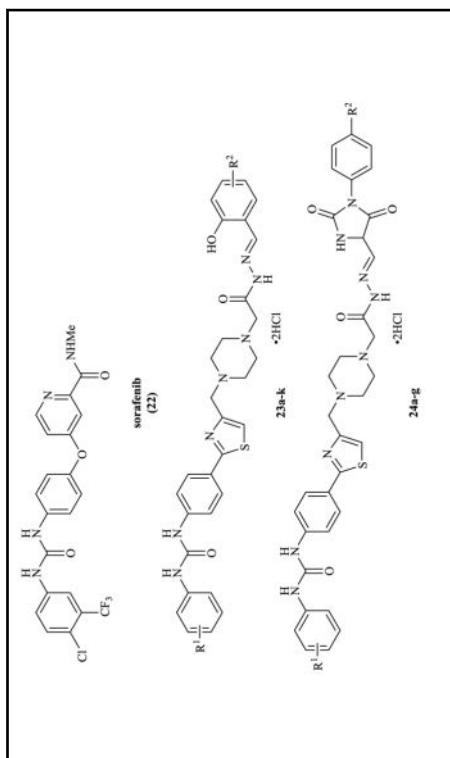
Compound	Zn ²⁺ K _d (nM)	% Caspase-3 Activation at 10 μM	U-937 72h IC ₅₀ (μM)
PAC-1	52 ± 2	45.8 ± 4.8	4.8 ± 1.0
<i>Class I</i>			
2	77 ± 2	30 ± 2	15.3 ± 2.0
3	> 10 ⁴	0	> 100
11a	> 10 ⁴	0	> 100
11b	> 10 ⁴	0	> 100
11c	> 10 ⁴	0	> 100
11d	> 10 ⁴	0	> 100
11e	> 10 ⁴	0	
11f	> 10 ⁴	0	> 100
11g	43 ± 9	59 ± 5	1.8 ± 0.4
11h	> 10 ⁴	0	32 ± 12
12	> 10 ⁴	0	> 100
<i>Class II</i>			
13a	68 ± 10	48 ± 3	9.5 ± 1.8
13b	62 ± 9	20.6 ± 1.6	14 ± 2
13c	80 ± 14	26.3 ± 0.1	21 ± 6
14a	48 ± 3	24.2 ± 1.7	2.0 ± 0.2
14b	39 ± 3	31 ± 3.6	1.0 ± 0.1
14c	47 ± 5	24 ± 3.4	2.7 ± 0.8
14d	45 ± 13	19.5 ± 1.8	4.6 ± 1.0
<i>Class III</i>			
15	65 ± 4	30.7 ± 1.2	12 ± 2
<i>Class IV</i>			
16a	44 ± 2	0 ^a	2.8 ± 1.1
16b	48 ± 7	0 ^a	6.5 ± 3.6
17a	> 10 ⁴	4.4 ± 0.9	> 100
17b	> 10 ⁴	4.1 ± 1.0	> 100
18	49 ± 2	36 ± 3	2.7 ± 1.1
19	> 10 ⁴	17.1 ± 1.2	59 ± 14
20	> 10 ⁴	0	22 ± 3

^a – These derivatives slightly inhibited caspase-3, masking any activation. [43]

Table 2

Structure and cytotoxicity of hybrid **PAC-1**/sorafenib derivatives.

Compound	R ¹	R ²	IC ₅₀ (μM)			
			A549	HL-60	MDA-MB-231	
23a	3-F	5-Br	2.3	7.1	1.4	
23b	3-F	3,4-F ₂	1.9	6.2	1.1	
23c	3-F	3,5-(<i>t</i> -Bu) ₂	> 100	1.1	23	
23d	2-Cl-4-CF ₃	-	2.0	9.9	1.4	
23e	3-Cl	5-Cl	4.4	6	1.6	
23f	3-Cl	3,5-(<i>t</i> -Bu) ₂	0.7	2.7	1.0	
23g	3-Cl	4-Me	> 100	1.2	> 100	
23h	3-F	4-OBn	1.1	1.1	1.0	
23i	3-F	4-OCH ₂ (4-Cl-Ph)	0.8	2.8	0.8	
23j	3-F	4-OCH ₂ (2,4-Cl ₂ -Ph)	0.7	0.13	0.5	
23k	3-F	4-OCH ₂ (3-F-Ph)	0.9	1.6	0.7	
24a	3-F	Me	18	32	93	
24b	3-F	Cl	12	22	31	
24c	3-Cl	Me	73	24	14	



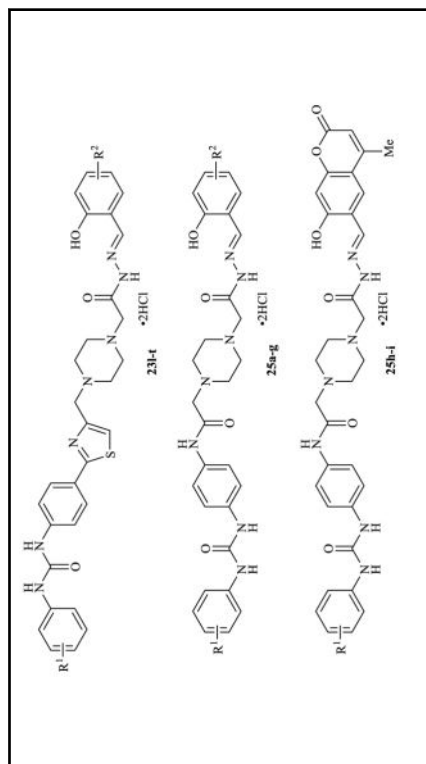
Compound	R ¹	R ²	IC ₅₀ (μM)			
			A549	HL-60	MDA-MB-231	
24d	3-OMe	CF ₃	> 100	> 100	> 100	> 100
24e	2-Cl-4-CF ₃	CF ₃	> 100	30	> 100	> 100
24f	3,5-(CF ₃) ₂	CF ₃	12	12	31	31
24g	3,4-F ₂	CF ₃	3.5	6.2	3.0	3.0
Sorafenib	-	-	2.6	N.D.	5.4	5.4
PAC-1	-	-	5.6	9.1	4.1	4.1

N.D. = not determined. [52]

Table 3

Structure and cytotoxicity of hybrid **PAC-1**/sorafenib derivatives.

Compound	R ¹	R ²	IC ₅₀ (μM)				
			A549	HL-60	MDA-MB-231	WI-38	
23l	2-CF ₃	-	3.88	2.40	4.65	11.67	
23m	2,4-Cl ₂	-	2.40	0.33	1.27	N.D.	
23n	3-OCF ₃	3,5-(<i>i</i> -Bu) ₂	1.49	2.11	0.90	N.D.	
23o	-	5-OBn	1.67	0.55	0.74	N.D.	
23p	2-Cl-4-CF ₃	5-OBn	2.30	1.03	0.59	N.D.	
23q	2-OCF ₃	5-OBn	0.41	0.23	0.24	4.53	
23r	2-CF ₃	5-OBn	0.45	0.35	0.30	N.D.	
23s	3-Cl	4-OBn	0.83	1.18	0.52	6.91	
23t	3,4-Cl ₂	4-OBn	0.78	0.80	0.47	N.D.	
25a	3-CF ₃	-	8.97	4.24	2.39	N.D.	
25b	3-CF ₃	3,5-(<i>i</i> -Bu) ₂	1.34	1.29	0.49	N.D.	
25c	3-Cl	-	52.0	2.44	1.18	N.D.	
25d	3-CF ₃ -4-Cl	-	10.7	4.42	1.07	N.D.	
25e	3-CF ₃	5-OBn	3.16	2.66	1.48	N.D.	



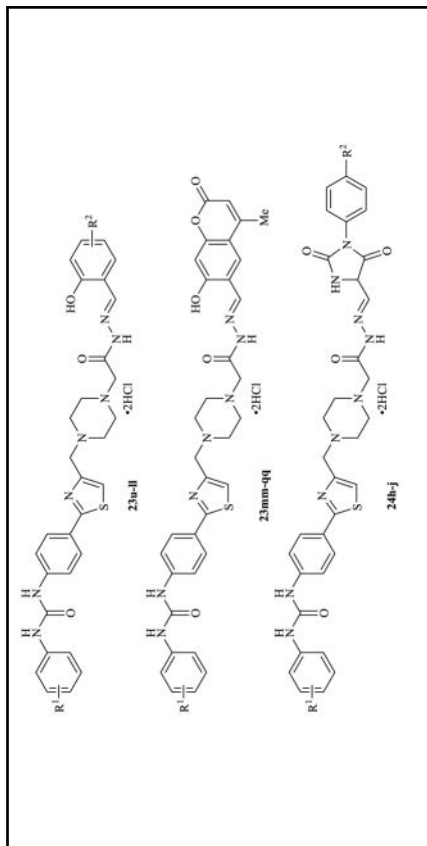
Compound	R ¹	R ²	IC ₅₀ (μM)				
			A549	HL-60	MDA-MB-231	WT-38	
25f	3-Cl	5-OBn	> 100	1.70	> 100	N.D.	
25g	3-CF ₃ -4-Cl	5-OBn	4.02	1.82	1.92	N.D.	
25h	3-CF ₃	-	18.0	5.54	> 100	N.D.	
25i	3-Cl-4-CF ₃	-	> 100	3.08	8.92	N.D.	
Sorafenib	-	-	1.30	N.D.	2.70	10.8	
PAC-1	-	-	2.81	4.56	2.04	6.63	

N.D. = not determined. [53]

Table 4

Structure and cytotoxicity of hybrid PAC-1/sorafenib derivatives.

Compound	R ¹	R ²	72h IC ₅₀ (μM)			
			A549	HL-60	MDA-MB-231	
23u	3-F	4-Me	0.64 ± 0.12	N.D.	1.9 ± 0.16	
23v	3,5-Cl ₂	4-CH ₂ C(=CH ₂)Me	0.78 ± 0.02	0.56 ± 0.04	0.48 ± 0.02	
23w	3-Cl-4-F	3,5-(<i>t</i> -Bu) ₂	0.48 ± 0.06	13.0 ± 0.37	0.26 ± 0.01	
23x	4-CF ₃	3-Me-6- <i>i</i> Pr	5.1 ± 0.25	8.8 ± 0.31	8.5 ± 0.44	
23y	4-CF ₃	5- <i>t</i> Bu	1.6 ± 0.41	0.82 ± 0.08	0.92 ± 0.24	
23z	4-CF ₃	5-OMe	1.3 ± 0.16	0.63 ± 0.17	0.82 ± 0.05	
23aa	3-CF ₃	-	0.50 ± 0.04	6.0 ± 0.09	0.58 ± 0.03	
23bb	3-Cl	4-OCH ₂ (4-Cl-Ph)	0.59 ± 0.02	2.6 ± 0.11	0.71 ± 0.01	
23cc	3-Cl	4-OCH ₂ (2,4-Cl ₂ -Ph)	1.7 ± 0.12	3.8 ± 0.13	0.53 ± 0.02	
23dd	3,4-Cl ₂	4-OCH ₂ (3-F-Ph)	0.49 ± 0.05	2.3 ± 0.11	0.35 ± 0.02	
23ee	3,4-Cl ₂	4-OCH ₂ (4-Cl-Ph)	2.8 ± 0.21	4.7 ± 0.19	0.48 ± 0.05	
23ff	3-F	5-OBn	1.6 ± 0.14	0.55 ± 0.09	0.73 ± 0.06	
23gg	3-Cl	5-OBn	1.2 ± 0.05	0.51 ± 0.01	0.73 ± 0.02	
23hh	3-OCF ₃	5-OCH ₂ (2-F-Ph)	0.34 ± 0.01	0.22 ± 0.01	0.41 ± 0.3	



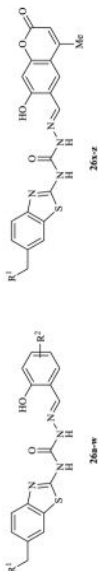
Compound	R ¹	R ²	72h IC ₅₀ (μM)			
			A549	HL-60	MDA-MB-231	
23ii	-	5-OCH ₂ (2-F-Ph)	1.8 ± 0.04	0.50 ± 0.004	0.90 ± 0.006	
23jj	2-CF ₃	5-OCH ₂ (4-Cl-Ph)	0.54 ± 0.06	0.38 ± 0.01	0.44 ± 0.4	
23kk	3-CF ₃ -4-Cl	5-OCH ₂ (2-F-Ph)	0.96 ± 0.20	0.31 ± 0.14	2.0 ± 0.12	
23ll	3-Cl-4-F	5-OCH ₂ (3-Cl-Ph)	2.3 ± 0.08	2.0 ± 0.11	0.22 ± 0.04	
23mm	-	-	17.0 ± 0.52	15.2 ± 0.22	5.6 ± 0.36	
23nn	3-CF ₃	-	> 50	3.6 ± 0.12	3.8 ± 0.28	
23oo	3-OMe	-	6.4 ± 0.42	3.3 ± 0.25	3.6 ± 0.28	
23pp	3,5-(CF ₃) ₂	-	1.7 ± 0.15	4.0 ± 0.33	1.8 ± 0.07	
23qq	3,4-Me ₂	-	19.0 ± 0.57	4.5 ± 0.13	8.9 ± 0.41	
24h	3-Cl-4-CF ₃	CF ₃	37.2 ± 0.46	12.0 ± 0.32	7.0 ± 0.18	
24i	3-CF ₃	CF ₃	3.4 ± 0.10	25.5 ± 0.29	13.3 ± 0.32	
24j	3-CF ₃	F	7.8 ± 0.20	> 50	13.1 ± 0.37	
Sorafenib	-	-	1.3 ± 0.06	N.D.	2.7 ± 0.11	
PAC-1	-	-	2.8 ± 0.10	4.5 ± 0.03	2.0 ± 0.05	

N.D. = not determined. [54]

Table 5

Structure and cytotoxicity of benzothiazole PAC-1 derivatives.

Compound	R ¹	R ²	72h IC ₅₀ (μM)				
			HT-29	MDA-MB-231	MKN-45	NCI-H226	SK-N-SH
26a	NMe ₂	3-All	N.D.	3.55 ± 0.17	1.01 ± 0.15	N.D.	1.68 ± 0.11
26b	NMe ₂	3,5-(<i>t</i> Bu) ₂	N.D.	13.9 ± 0.24	2.48 ± 0.08	N.D.	2.28 ± 0.04
26c	NEt ₂	3-All	N.D.	5.25 ± 0.19	1.80 ± 0.12	N.D.	2.10 ± 0.09
26d	NEt ₂	3,5-(<i>t</i> Bu) ₂	N.D.	7.23 ± 1.01	4.06 ± 1.26	N.D.	2.46 ± 0.21
26e	4-Me-1-Pip	3-All	N.D.	3.11 ± 0.31	1.31 ± 0.22	N.D.	2.58 ± 0.12
26f	4-Me-1-Pip	3,5-(<i>t</i> Bu) ₂	N.D.	12.1 ± 0.15	9.70 ± 0.26	N.D.	2.79 ± 0.13
26g	NMe ₂	4-OBn	2.19 ± 0.17	1.34 ± 0.11	1.06 ± 0.10	0.91 ± 0.03	1.14 ± 0.11
26h	NMe ₂	4-OCH ₂ (4-F-Ph)	1.32 ± 0.07	2.02 ± 0.01	1.72 ± 0.04	0.42 ± 0.05	0.88 ± 0.03
26i	NMe ₂	4-OCH ₂ (3-F-Ph)	1.03 ± 0.12	2.02 ± 0.12	1.35 ± 0.04	0.51 ± 0.03	1.29 ± 0.08
26j	NMe ₂	4-OCH ₂ (2-F-Ph)	1.51 ± 0.04	0.66 ± 0.02	0.35 ± 0.03	0.59 ± 0.01	1.94 ± 0.15
26k	NMe ₂	4-OCH ₂ (4-CF ₃ -Ph)	0.92 ± 0.08	0.63 ± 0.03	0.29 ± 0.01	0.24 ± 0.02	0.60 ± 0.02
26l	NMe ₂	4-OCH ₂ (2,4-Cl ₂ -Ph)	N.D.	2.02 ± 0.13	1.38 ± 0.05	0.50 ± 0.04	0.59 ± 0.01
26m	NMe ₂	4-OCH ₂ (2,3-Cl ₂ -Ph)	N.D.	2.94 ± 0.08	1.45 ± 0.03	0.81 ± 0.01	0.87 ± 0.02
26n	NEt ₂	4-OCH ₂ (4-F-Ph)	1.47 ± 0.03	0.97 ± 0.08	0.31 ± 0.07	0.57 ± 0.07	0.71 ± 0.06
26o	NEt ₂	4-OCH ₂ (3-F-Ph)	0.76 ± 0.02	1.12 ± 0.11	0.63 ± 0.10	1.05 ± 0.03	1.34 ± 0.05
26p	NEt ₂	4-OCH ₂ (2-F-Ph)	1.06 ± 0.12	0.88 ± 0.02	0.55 ± 0.02	0.62 ± 0.06	0.91 ± 0.15
26q	NEt ₂	4-OCH ₂ (4-CF ₃ -Ph)	1.59 ± 0.14	1.06 ± 0.05	0.57 ± 0.01	0.54 ± 0.04	0.85 ± 0.02
26r	NEt ₂	4-OCH ₂ (2,3-Cl ₂ -Ph)	4.01 ± 0.27	1.74 ± 0.02	0.71 ± 0.05	0.95 ± 0.02	1.41 ± 0.13
26s	4-Me-1-Pip	4-OCH ₂ (4-F-Ph)	4.01 ± 0.18	2.37 ± 0.04	0.79 ± 0.12	0.31 ± 0.03	0.40 ± 0.01
26t	4-Me-1-Pip	4-OCH ₂ (3-F-Ph)	1.02 ± 0.11	0.83 ± 0.05	0.38 ± 0.01	0.36 ± 0.04	0.56 ± 0.09



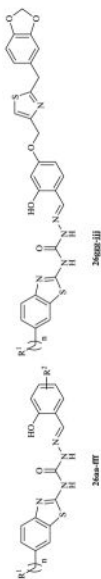
Compound	R ¹	R ²	72h IC ₅₀ (μM)					
			HT-29	MDA-MB-231	MKN-45	NCI-H226	SK-N-SH	
26u	4-Me-1-Pip	4-OCH ₂ (2-F-Ph)	1.65 ± 0.13	0.42 ± 0.01	0.40 ± 0.02	0.45 ± 0.05	1.38 ± 0.11	
26v	4-Me-1-Pip	4-OCH ₂ (4-CF ₃ -Ph)	1.12 ± 0.06	0.58 ± 0.03	0.31 ± 0.02	0.65 ± 0.11	0.75 ± 0.08	
26w	4-Me-1-Pip	4-OCH ₂ (2,3-Cl ₂ -Ph)	3.34 ± 0.18	1.00 ± 0.11	0.45 ± 0.07	0.33 ± 0.05	0.55 ± 0.09	
26x	NMe ₂	-	N.D.	16.18 ± 0.55	5.32 ± 0.12	N.D.	6.12 ± 1.12	
26y	NEt ₂	-	N.D.	12.7 ± 0.36	5.83 ± 0.48	N.D.	4.37 ± 0.69	
26z	4-Me-1-Pip	-	N.D.	10.49 ± 1.05	4.35 ± 1.08	N.D.	2.72 ± 0.15	
PAC-1	-	-	1.36 ± 0.02	4.58 ± 0.05	3.56 ± 0.05	1.02 ± 0.08	3.06 ± 0.16	

Pip = piperidinyl; N.D. = not determined. [57]

Table 6

Structure and cytotoxicity of benzothiazole PAC-1 derivatives.

Compound	\bar{n}	R^1	R^2	72h IC ₅₀ (μM)							
				HT-29	MDA-MB-231	MKN-45	NCI-H226	SK-N-SH			
26aa	1	NMe ₂	-	5.96 ± 0.52	5.95 ± 0.21	1.54 ± 1.01	2.03 ± 0.38	5.14 ± 1.02			
26bb	1	NMe ₂	4-OH	77.92 ± 5.40	> 100	2.85 ± 0.13	2.98 ± 0.34	14.31 ± 1.35			
26cc	1	NEt ₂	-	4.03 ± 0.54	11.33 ± 0.23	1.71 ± 0.08	1.81 ± 0.11	5.79 ± 1.01			
26dd	1	NEt ₂	4-OH	23.73 ± 1.67	4.11 ± 0.16	1.74 ± 0.26	5.16 ± 0.19	6.05 ± 0.17			
26ee	1	4-Me-1-Pip	-	10.40 ± 2.62	12.29 ± 0.03	0.68 ± 0.06	2.96 ± 0.28	4.36 ± 1.52			
26ff	1	4-Me-1-Pip	4-OH	2.73 ± 0.05	1.66 ± 0.31	4.09 ± 0.16	4.61 ± 0.15	7.74 ± 1.26			
26gg	1	4-Morph	-	10.32 ± 1.06	12.04 ± 1.21	2.34 ± 0.32	2.71 ± 0.18	7.05 ± 0.76			
26hh	0	4-Morph	-	67.93 ± 2.11	> 100	9.31 ± 0.51	4.26 ± 0.11	11.68 ± 0.78			
26ii	1	NMe ₂	4-OCH ₂ (4-Me-Ph)	2.13 ± 0.04	2.65 ± 0.02	1.27 ± 0.02	1.08 ± 0.05	2.58 ± 0.11			
26jj	1	NMe ₂	4-OCH ₂ (4- <i>t</i> -Bu-Ph)	1.51 ± 0.11	1.14 ± 0.01	1.04 ± 0.01	0.83 ± 0.17	1.66 ± 0.15			
26kk	1	NMe ₂	4-OCH ₂ (4-Cl-Ph)	2.15 ± 0.18	0.60 ± 0.05	0.70 ± 0.09	1.17 ± 0.10	2.74 ± 0.12			
26ll	1	NMe ₂	4-OCH ₂ (3-Cl-Ph)	2.94 ± 0.11	0.54 ± 0.04	0.19 ± 0.01	0.36 ± 0.07	1.19 ± 0.18			
26mm	1	NMe ₂	4-OCH ₂ (2-Cl-Ph)	1.61 ± 0.25	0.68 ± 0.12	0.33 ± 0.01	0.58 ± 0.01	2.94 ± 0.15			
26nn	1	NEt ₂	4-OCH ₂ (4-Me-Ph)	1.33 ± 0.13	0.71 ± 0.03	0.58 ± 0.01	1.01 ± 0.02	1.43 ± 0.09			
26oo	1	NEt ₂	4-OCH ₂ (4- <i>t</i> -Bu-Ph)	0.77 ± 0.01	0.98 ± 0.03	0.50 ± 0.02	0.16 ± 0.01	0.48 ± 0.02			
26pp	1	NEt ₂	4-OCH ₂ (4-Cl-Ph)	1.02 ± 0.02	0.61 ± 0.01	0.54 ± 0.08	0.43 ± 0.01	0.74 ± 0.05			
26qq	1	NEt ₂	4-OCH ₂ (3-Cl-Ph)	1.88 ± 0.01	0.57 ± 0.02	0.42 ± 0.02	1.30 ± 0.14	1.83 ± 0.13			
26rr	1	NEt ₂	4-OCH ₂ (2-Cl-Ph)	2.23 ± 0.16	0.74 ± 0.03	0.42 ± 0.01	0.56 ± 0.10	2.01 ± 0.01			
26ss	1	NEt ₂	4-OCH ₂ (2,4-Cl ₂ -Ph)	2.43 ± 0.03	1.52 ± 0.03	0.52 ± 0.03	0.70 ± 0.02	1.04 ± 0.05			
26tt	1	NEt ₂	4-OBn	1.44 ± 0.23	N.D.	N.D.	0.88 ± 0.01	1.67 ± 0.07			
26uu	1	4-Me-1-Pip	4-OCH ₂ (4-Me-Ph)	1.04 ± 0.03	1.51 ± 0.02	0.31 ± 0.02	1.06 ± 0.05	1.56 ± 0.02			

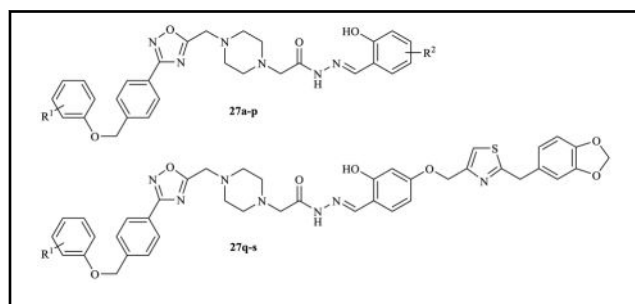


Compound	n	R ¹	R ²	72h IC ₅₀ (μM)					
				HT-29	MDA-MB-231	MKN-45	NCI-H226	SK-N-SH	
26vv	1	4-Me-1-Pip	4-OCH ₂ (4-t-Bu-Ph)	0.87 ± 0.03	0.56 ± 0.01	0.17 ± 0.02	0.18 ± 0.02	0.27 ± 0.03	
26vvv	1	4-Me-1-Pip	4-OCH ₂ (4-Cl-Ph)	0.95 ± 0.10	0.88 ± 0.03	0.21 ± 0.01	0.41 ± 0.06	1.06 ± 0.07	
26xx	1	4-Me-1-Pip	4-OCH ₂ (3-Cl-Ph)	1.72 ± 0.04	1.12 ± 0.02	0.67 ± 0.09	0.36 ± 0.03	0.34 ± 0.01	
26yy	1	4-Me-1-Pip	4-OCH ₂ (2-Cl-Ph)	1.03 ± 0.14	2.3 ± 0.05	0.76 ± 0.06	0.79 ± 0.06	0.85 ± 0.07	
26zz	1	4-Me-1-Pip	4-OCH ₂ (2,4-Cl ₂ -Ph)	1.00 ± 0.09	0.30 ± 0.03	0.28 ± 0.03	0.39 ± 0.06	1.03 ± 0.19	
26aaa	1	4-Me-1-Pip	4-OBn	1.57 ± 0.02	N.D.	N.D.	0.61 ± 0.11	1.32 ± 0.05	
26bbb	0	4-Morph	4-OCH ₂ (4-Me-Ph)	1.58 ± 0.17	19.34 ± 0.31	0.75 ± 0.03	0.53 ± 0.05	2.51 ± 0.15	
26ccc	0	4-Morph	4-OCH ₂ (4-t-Bu-Ph)	0.92 ± 0.15	1.04 ± 0.05	0.46 ± 0.04	0.24 ± 0.03	0.92 ± 0.33	
26ddd	0	4-Morph	4-OCH ₂ (4-Cl-Ph)	0.0018 ± 0.0002	4.46 ± 0.03	0.29 ± 0.01	0.26 ± 0.01	1.37 ± 0.03	
26eee	0	4-Morph	4-OCH ₂ (3-Cl-Ph)	0.59 ± 0.04	1.18 ± 0.01	0.28 ± 0.02	0.79 ± 0.11	1.48 ± 0.13	
26fff	0	4-Morph	4-OCH ₂ (2,4-Cl ₂ -Ph)	4.72 ± 0.13	15.06 ± 1.01	1.75 ± 0.10	1.22 ± 0.23	3.14 ± 0.08	
26ggg	1	NMe ₂	-	1.88 ± 0.03	1.04 ± 0.11	0.62 ± 0.01	0.72 ± 0.03	0.79 ± 0.01	
26hhh	1	NEt ₂	-	0.72 ± 0.02	0.55 ± 0.01	0.51 ± 0.01	0.14 ± 0.01	0.48 ± 0.03	
26iii	1	4-Me-1-Pip	-	1.12 ± 0.15	0.88 ± 0.02	0.55 ± 0.03	0.81 ± 0.02	1.25 ± 0.01	
26jjj	0	4-Morph	-	2.31 ± 0.16	4.03 ± 0.04	1.01 ± 0.01	2.14 ± 0.11	6.21 ± 0.23	
PAC-1	-	-	-	1.36 ± 0.02	4.8 ± 0.02	2.61 ± 0.05	1.02 ± 0.01	3.06 ± 0.04	

Pip = piperidinyli; Morph = morpholine; N.D. = not determined. [58]

Table 7

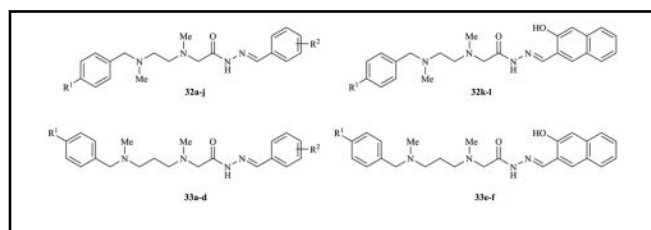
Structure and cytotoxicity of oxadiazole-containing PAC-1 derivatives. [48, 49]



Compound	R ¹	R ²	HL-60 72h IC ₅₀ (μM)
27a	4-Cl	3-All	0.25
27b	4-F	3-All	0.39
27c	3-Cl	3-All	0.40
27d	2-CF ₃	3-All	0.35
27e	4-Cl	4-OBn	1.26
27f	4-F	4-OCH ₂ (2,4-Cl ₂ -Ph)	1.02
27g	4-F	4-OCH ₂ (3-CF ₃ -Ph)	0.98
27h	4-Cl	4-OCH ₂ (4- <i>t</i> -Bu-Ph)	0.67
27i	4-Cl	4-OCH ₂ (2,4-Cl ₂ -Ph)	1.07
27j	4-F	4-OCH ₂ (4- <i>t</i> -Bu-Ph)	0.60
27k	3,4-F ₂	4-OBn	0.34
27l	3,4-F ₂	4-OCH ₂ (4-Cl-Ph)	0.30
27m	3,4-F ₂	4-OCH ₂ (2,4-Cl ₂ -Ph)	0.41
27n	2-CF ₃	4-OCH ₂ (4- <i>t</i> -Bu-Ph)	0.40
27o	2-CF ₃	4-OCH ₂ (3-F-Ph)	1.93
27p	4-Cl	4-OCH ₂ (3-Cl-Ph)	> 20
27q	2-CF ₃	-	1.08
27r (WF-208)	4-Cl	-	0.08
27s (WF-210)	4-F	-	0.08
PAC-1	-	-	4.03

Table 8

Structure and cytotoxicity of ethylenediamine and propylenediamine PAC-1 derivatives.



Compound	R ¹	R ²	72h IC ₅₀ (μM)	
			HL-60	HLF
32a	H	2-OH	3.63 ± 0.32	3.02 ± 0.58
32b	H	2-OH-3-All	2.32 ± 0.41	3.36
32c	H	2-OH-4-NEt ₂	0.27 ± 0.12	0.17 ± 0.13
32d	H	3-OH	183.51 ± 5.52	N.D.
32e	<i>t</i> -Bu	2-OH-3-All	0.73 ± 0.57	0.9 ± 0.01
32f	<i>t</i> -Bu	2-OH-3,5-(<i>t</i> -Bu) ₂	0.82 ± 0.22	0.98 ± 0.12
32g	<i>t</i> -Bu	2-OH-4-NEt ₂	0.25 ± 0.15	0.86 ± 0.04
32h	<i>t</i> -Bu	3-OH	11.65 ± 3.42	111.37 ± 0.45
32i	OMe	2-OH-3,5-(<i>t</i> -Bu) ₂	0.91 ± 0.17	1.07 ± 0.31
32j	OMe	2-OH-4-NEt ₂	0.30 ± 0.08	1.80 ± 0.95
32k	<i>t</i> -Bu	-	0.28 ± 0.03	1.86 ± 0.04
32l	OMe	-	0.56 ± 0.36	1.39 ± 0.30
33a	H	2-OH-3,5-(<i>t</i> -Bu) ₂	0.85 ± 0.02	0.87 ± 0.03
33b	<i>t</i> -Bu	2-OH-4-NEt ₂	0.26 ± 0.06	25.13 ± 3.01
33c	OMe	2-OH-3,5-(<i>t</i> -Bu) ₂	0.54 ± 0.13	1.15 ± 0.18
33d	OMe	2-OH-4-NEt ₂	0.46 ± 0.22	0.37
33e	<i>t</i> -Bu	-	0.28 ± 0.07	0.29 ± 0.06
33f	OMe	-	0.71 ± 0.31	N.D.
PAC-1	-	-	1.90 ± 0.01	5.82 ± 0.58

N.D. = not determined. [64]

Table 9Cytotoxicity of **PAC-1** and derivative **33b** against a panel of human cell lines. [64]

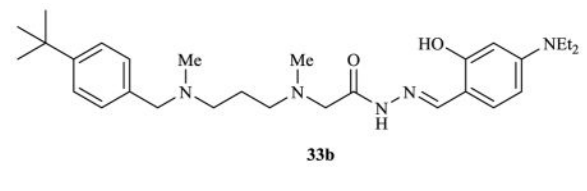
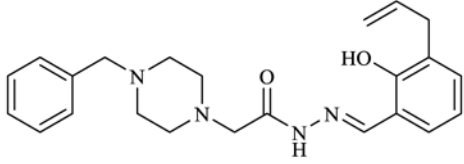
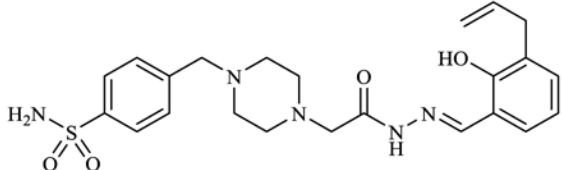
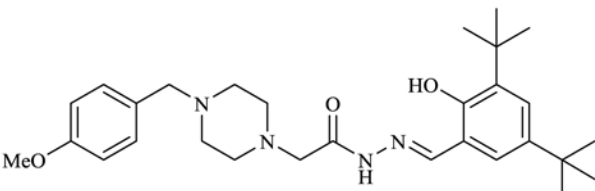
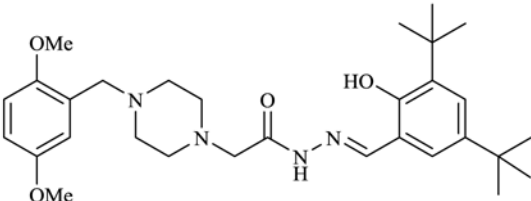
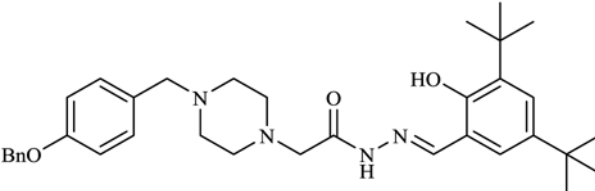
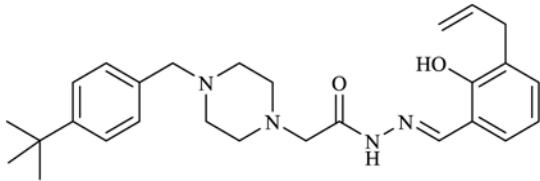
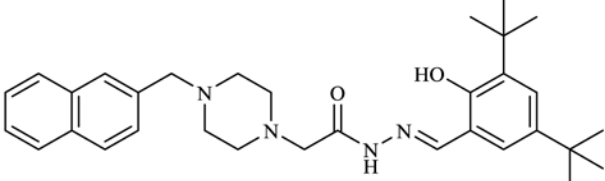
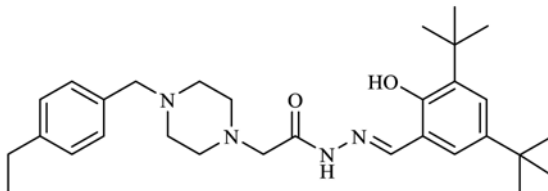
 33b			
		72h IC₅₀ (μM)	
Cell Line	Origin	PAC-1	33b
A-498	Renal	> 300	7.26 ± 1.56
A2780	Ovarian	56.02 ± 3.46	20.37 ± 4.13
BGC-823	Gastric	3.02 ± 1.01	0.35 ± 0.03
Caco-2	Colon	6.49 ± 1.35	1.35 ± 0.32
DU145	Prostate	> 300	25.29 ± 4.58
HCT-8	Colon	1.48 ± 0.24	0.18 ± 0.04
HeLa	Cervical	7.25 ± 2.31	1.50 ± 0.28
Hep G2	Liver	7.26 ± 1.43	1.05 ± 0.04
HL-60	Leukemia	1.90 ± 0.01	0.26 ± 0.06
HOS	Osteosarcoma	2.82 ± 0.05	0.79 ± 0.06
IM-9	Multiple Myeloma	1.87 ± 0.05	0.15 ± 0.01
K562	Leukemia	45.87 ± 3.65	3.00 ± 1.21
MCF7	Breast	> 300	14.76 ± 2.67
NCI-H460	Lung	4.16 ± 0.33	1.21 ± 0.42
SH-SY5Y	Neuroblastoma	13.93 ± 2.21	1.20 ± 0.01
HLF	Lung Fibroblast	5.82 ± 0.58	25.13 ± 3.01

Table 10

Six library compounds induce potent cell death of U-937 cells (human lymphoma) in both 24-h^a and 72-h^b experiments and enhance enzymatic activity of procaspase-3 *in vitro*.^c

Compound	U-937 72h IC ₅₀ (μ M)	U-937 %Cell Death (24h, 7.5 μ M)	%Procaspase-3 Activity (25 μ M)
 PAC-1 (1)	3.8 \pm 0.4	21	42 \pm 1.8
 S-PAC-1 (37)	4.4 \pm 0.7	23	4 \pm 0.6
 36{2,7}	1.8 \pm 0.2	90	53 \pm 4.1
 36{4,7}	1.6 \pm 0.2	53	64 \pm 2.5
 B-PAC-1 (36{18,7})	1.4 \pm 0.2	97	36 \pm 1.6

Compound	U-937 72h IC ₅₀ (μ M)	U-937 %Cell Death (24h, 7.5 μ M)	%Procaspase-3 Activity (25 μ M)
 36 {20,24}	0.9 \pm 0.03	83	82 \pm 2.4
 36 {25,7}	1.0 \pm 0.04	50	69 \pm 5.3
 36 {28,7}	2.0 \pm 0.2	70	60 \pm 2.4

^aCell viability determined by Annexin V-FITC/propidium iodide staining.

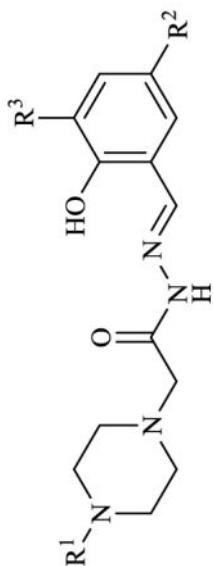
^bBiomass quantified using the sulforhodamine B assay.

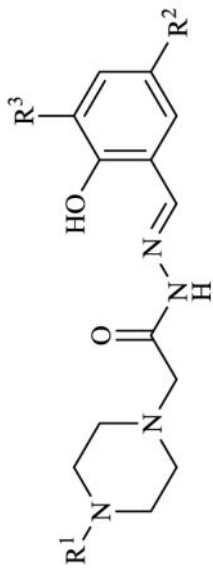
^cCompounds were tested at a concentration of 50 μ M with 1 μ M procaspase-3 (wild-type) and 3.5 μ M ZnSO₄. Cleavage of the Ac-DEVD-pNA substrate was monitored at 405 nm and normalized to a DMSO-treated control (0%) and a zinc-free control (100%). [46]

Table 11

Cytotoxicity,^a metabolic stability,^b and mouse toxicity^c of PAC-1 analogues.

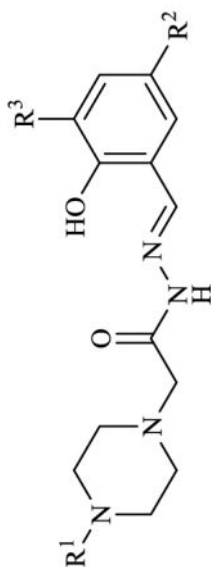
Compound	R ¹	R ²	R ³	U-937 72h IC ₅₀ (nM)	RLM 3h %Stability	Mouse Toxicity IP 200 mg/kg (* = 100 mg/kg)
PAC-1 (I)	Bn	H	All	10.2 ± 0.3	38 ± 2	Severe
14a	4-F-Bn	H	All	11.1 ± 2.1	31 ± 1	N.D.
S-PAC-1 (37)	4-SO ₂ NH ₂ -Bn	H	All	8.9 ± 0.6	84 ± 1	None
38	Bz	H	All	12.1 ± 1.3	89 ± 4	N.D.
39	4-CN-Bn	H	All	13.7 ± 0.9	48 ± 2	N.D.
40	4-CN-Bz	H	All	13.1 ± 3.7	90 ± 4	N.D.
41	4-F-Bz	H	All	10.2 ± 1.7	86 ± 2	Moderate
42	4-CF ₃ -Bn	H	All	15.3 ± 6.7	16 ± 1	N.D.
43	4-CF ₃ -Bz	H	All	6.6 ± 1.9	85 ± 6	Lethal*
44	Bn	H	<i>n</i> -Pr	9.6 ± 2.1	30 ± 1	N.D.
45	4-SO ₂ NH ₂ -Bn	H	<i>n</i> -Pr	4.9 ± 0.4	61 ± 2	N.D.
46	Bz	H	<i>n</i> -Pr	9.4 ± 1.3	71 ± 3	N.D.
47	4-CN-Bn	H	<i>n</i> -Pr	9.0 ± 1.2	30 ± 2	N.D.
48	4-CN-Bz	H	<i>n</i> -Pr	12.8 ± 2.7	61 ± 3	N.D.
49	4-F-Bn	H	<i>n</i> -Pr	10.0 ± 1.7	24 ± 2	N.D.
50	4-F-Bz	H	<i>n</i> -Pr	7.3 ± 0.9	69 ± 4	N.D.
51	4-CF ₃ -Bn	H	<i>n</i> -Pr	4.1 ± 0.4	15 ± 2	N.D.
52	4-CF ₃ -Bz	H	<i>n</i> -Pr	4.8 ± 1.2	64 ± 1	Lethal*
53	Bn	F	H	17.0 ± 1.4	64 ± 4	N.D.





Compound	R ¹	R ²	R ³	U-937 72h IC ₅₀ (μM)	RLM 3h %Stability	Mouse Toxicity IP 200 mg/kg (* = 100 mg/kg)
54	4-SO ₂ NH ₂ -Bn	F	H	N.D.	N.D.	N.D.
55	Bz	F	H	15.7 ± 2.6	88 ± 1	N.D.
56	4-CN-Bn	F	H	N.D.	N.D.	N.D.
57	4-CN-Bz	F	H	15.3 ± 1.3	88 ± 4	N.D.
58	4-F-Bn	F	H	N.D.	N.D.	N.D.
59	4-F-Bz	F	H	15.3 ± 0.8	86 ± 2	N.D.
60	4-CF ₃ -Bn	F	H	4.7 ± 0.3	30 ± 5	N.D.
61	4-CF ₃ -Bz	F	H	8.7 ± 0.5	87 ± 3	Moderate
62	Bn	F	All	9.5 ± 0.9	56 ± 1	N.D.
63	4-SO ₂ NH ₂ -Bn	F	All	9.8 ± 1.3	89 ± 3	Lethal
64	Bz	F	All	8.6 ± 2.0	93 ± 7	Moderate
65	4-CN-Bn	F	All	12.7 ± 2.0	65 ± 2	N.D.
66	4-CN-Bz	F	All	10.1 ± 2.0	95 ± 4	Mild
67	4-F-Bn	F	All	10.3 ± 4.1	57 ± 1	N.D.
68	4-F-Bz	F	All	8.5 ± 1.4	92 ± 3	Severe
69	4-CF ₃ -Bn	F	All	3.4 ± 0.6	49 ± 3	N.D.
70	4-CF ₃ -Bz	F	All	6.5 ± 0.6	90 ± 2	Moderate
71	Bn	F	<i>n</i> -Pr	8.9 ± 1.2	49 ± 6	N.D.
72	4-SO ₂ NH ₂ -Bn	F	<i>n</i> -Pr	8.7 ± 0.4	62 ± 3	N.D.
73	Bz	F	<i>n</i> -Pr	12.3 ± 1.0	86 ± 5	N.D.
74	4-CN-Bn	F	<i>n</i> -Pr	11.2 ± 0.9	49 ± 5	N.D.
75	4-CN-Bz	F	<i>n</i> -Pr	9.4 ± 1.2	66 ± 3	Mild

Compound	R ¹	R ²	R ³	U-937 72h IC ₅₀ (μM)	RLM 3h %Stability	Mouse Toxicity IP 200 mg/kg (* = 100 mg/kg)
76	4-F-Bn	F	<i>n</i> -Pr	7.5 ± 0.7	48 ± 1	N.D.
77	4-F-Bz	F	<i>n</i> -Pr	7.5 ± 1.4	67 ± 3	Severe
78	4-CF ₃ -Bn	F	<i>n</i> -Pr	3.9 ± 0.6	40 ± 1	N.D.
79	4-CF ₃ -Bz	F	<i>n</i> -Pr	5.2 ± 0.6	64 ± 5	Lethal



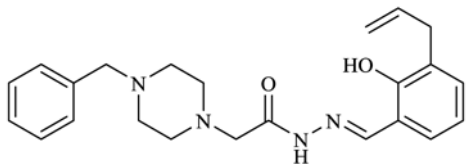
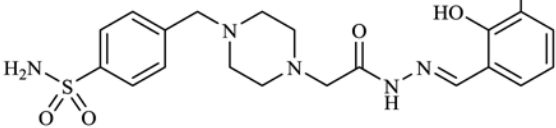
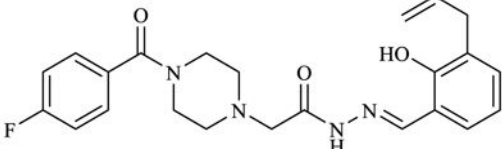
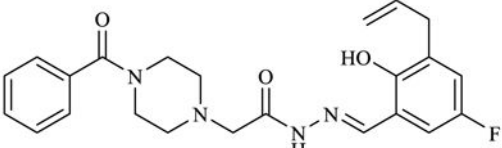
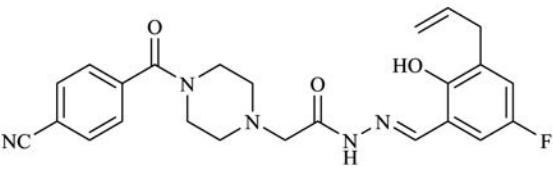
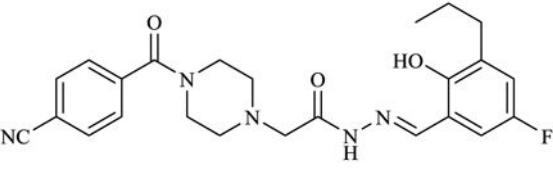
N.D. = not determined.

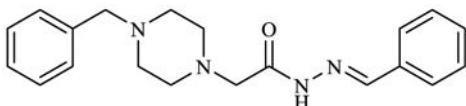
^a Cells treated with compounds for 72 hours. Biomass quantified by sulforhodamine B assay. IC₅₀ values shown are mean ± s.e.m. (n = 3).

^b Rat liver microsomes treated with compounds (10 μM) for 3 hours. Percent stability values shown are mean ± s.e.m. (n = 3).

^c Mice dosed with compound via i.p. injection at 200 mg/kg (except * 100 mg/kg). [50]

Table 12Zinc chelation^a and caspase activation^b by **PAC-1** derivatives.

Compound	Zn ²⁺ K _d (nM)	%Caspase-3/-7 Activity
 <p>PAC-1 (1)</p>	1.28 ± 0.03	87 ± 7
 <p>S-PAC-1 (37)</p>	2.72 ± 0.13	64 ± 11
 <p>41</p>	1.46 ± 0.07	64 ± 4
 <p>64</p>	1.07 ± 0.09	67 ± 6
 <p>66</p>	1.37 ± 0.10	83 ± 3
 <p>75</p>	1.37 ± 0.03	81 ± 4

Compound	Zn ²⁺ K _d (nM)	%Caspase-3/-7 Activity
 PAC-1a (3)	> 10 ⁶	3 ± 0.1

^aIncreasing amounts of Zn(OTf)₂ added to a buffered solution of EGTA (7.3 mM) and PAC-1 derivative (100 μM). K_d was determined by comparing fluorescence intensity (ex. 410 nm, em. 475 nm) and free zinc concentration.

^bU-937 cells treated with compounds (30 μM) for 16 hours, then lysed. Caspase-3/7 activity assessed by cleavage of fluorogenic substrate Ac-DEVD-AFC. [50]

PAC-1 and derivatives are cytotoxic to white blood cell cancer lines in culture. Cells treated with compounds for 72 hours. Biomass quantified by sulforhodamine B assay. IC_{50} values shown are mean \pm s.e.m. (n = 3). [50]

Table 13

Cell Line	Species	Origin	72h IC_{50} (μ M)					
			PAC-1	S-PAC-1	41	64	66	75
U-937	Human	Lymphoma	10.2 \pm 0.3	8.9 \pm 0.6	10.2 \pm 1.7	8.6 \pm 2.0	10.1 \pm 2.0	9.4 \pm 1.2
Jurkat	Human	Leukemia	4.4 \pm 0.6	4.5 \pm 1.2	4.0 \pm 0.5	4.1 \pm 0.7	3.5 \pm 0.2	3.4 \pm 0.6
GL-1	Dog	Lymphoma	3.0 \pm 0.1	3.2 \pm 0.2	3.0 \pm 0.1	3.4 \pm 0.2	2.4 \pm 0.4	2.2 \pm 0.3
OSW	Dog	Lymphoma	10.0 \pm 0.8	9.8 \pm 0.1	9.3 \pm 0.2	10.0 \pm 0.6	9.5 \pm 0.7	8.5 \pm 0.7
EL4	Mouse	Lymphoma	6.5 \pm 0.5	7.9 \pm 0.5	6.5 \pm 0.8	7.3 \pm 1.2	5.1 \pm 0.4	4.7 \pm 0.7

Table 14

Pharmacokinetic parameters for **PAC-1** and selected derivatives. 25 mg/kg dose was administered via intravenous injection or oral gavage. Values shown are mean \pm standard deviation (n = 2). [50]

Compound	$t_{1/2, IV}$ (min)	AUC_{IV} (min* μ g/mL)	AUC_{PO} (min* μ g/mL)	% F_{oral}
PAC-1	24.6 \pm 0.9	210.3 \pm 9.3	31.6 \pm 1.6	15.1 \pm 1.4
S-PAC-1	38.1 \pm 3.3	446.0 \pm 114.1	54.0 \pm 12.4	12.9 \pm 6.1
41	89.5 \pm 19.3	362.3 \pm 55.8	92.2 \pm 6.0	25.6 \pm 2.3
64	120.5 \pm 16.3	291.0 \pm 40.6	25.7 \pm 18.3	8.5 \pm 5.1
66	88.7 \pm 3.3	364.9 \pm 5.6	105.2 \pm 24.2	28.8 \pm 6.2
75	122.3 \pm 1.4	313.4 \pm 5.5	113.0 \pm 3.7	36.1 \pm 0.5

Table 15Comparison of cytotoxicity of **PAC-1** and **S-PAC-1**. Values shown are mean \pm s.e.m. (n = 3). [44]

Cell Line	Species	Origin	72h IC ₅₀ (μ M)	
			PAC-1	S-PAC-1
U-937	Human	Lymphoma	9.3 \pm 0.5	6.4 \pm 0.8
EL4	Mouse	Lymphoma	3.8 \pm 0.9	7.1 \pm 1.3
17-71	Dog	Lymphoma	2.5 \pm 0.9	2.7 \pm 0.8
GL-1	Dog	Lymphoma	4.9 \pm 0.3	7.1 \pm 0.3
OSW	Dog	Lymphoma	8.6 \pm 1.3	11.0 \pm 0.9
Jurkat	Human	Leukemia	5.7 \pm 2.8	4.5 \pm 1.1
SK-MEL-5	Human	Melanoma	11.5 \pm 3.6	8.6 \pm 1.3
HeLa	Human	Cervical	15.5 \pm 3.8	28.4 \pm 7.7
MDA-MB-231	Human	Breast	9.9 \pm 1.0	11.7 \pm 5.3

Table 16

Time-dependence of cytotoxicity of **S-PAC-1** in U-937 cells. Cells were treated with **S-PAC-1** for the indicated time, compound was washed out, and cell death was assessed 72 hours after initiation of treatment. Values shown are mean \pm s.e.m. (n = 3). [44]

Exposure Time (h)	U-937 S-PAC-1 72h IC ₅₀ (μ M)
1	> 100
3	> 100
6	> 100
9	20 \pm 12
12	9.7 \pm 1.1
24	5.9 \pm 1.0
48	5.6 \pm 0.8
72	6.4 \pm 0.8

Author Manuscript

Author Manuscript

Author Manuscript

Author Manuscript

Table 17

Potency of **PAC-1**, **WF-208**, and **WF-210** against a diverse array of human cancer cell lines in culture. [48, 49]

<u>Cell Line</u>	<u>Origin</u>	<u>72h IC₅₀ (μM)</u>		
		<u>PAC-1</u>	<u>WF-208</u>	<u>WF-210</u>
A549	Lung	25.48	0.42	1.78
COLO205	Colon	11.46	12.85	1.1
DU145	Prostate	26.03	0.08	0.08
GBC-SD	Gallbladder	53.44	0.08	0.08
Hep 3B	Liver	25.48	0.98	0.86
Hep G2	Liver	16.35	0.73	0.22
HGC-27	Gastric	13.18	0.52	0.99
HL-60	Leukemia	4.03	0.08	0.08
K-562	Leukemia	14.55	0.20	0.22
MCF7	Breast	12.65	0.32	2.8
MDA-MB-435S	Melanoma	14.49	0.76	1.24
NCI-H226	Lung	28.74	4.59	2.58
U-87 MG	Glioblastoma	8.82	1.67	1.05
PC-3	Prostate	20.13	1.28	0.08
U-937	Lymphoma	16.42	0.08	0.08